

High-Throughput Synthesis and Screening of Titania-Based Photocatalysts

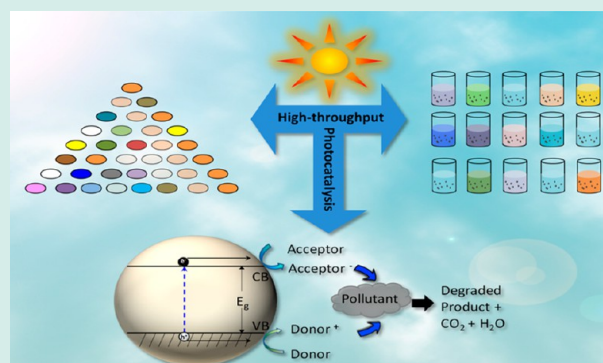
Natalita M. Nursam,^{†,§} Xingdong Wang,[§] and Rachel A. Caruso^{*,†,§}

[†]Particulate Fluids Processing Centre, School of Chemistry, The University of Melbourne, Melbourne, Victoria 3010, Australia

[§]CSIRO Manufacturing, Clayton, Victoria 3168, Australia

ABSTRACT: Titanium dioxide is widely known as a prominent photocatalyst material and research in this area has increased substantially over the last decades. However, the photoactivity of TiO₂ is hindered by several factors, such as a relatively high photogenerated electron–hole recombination rate and a wide bandgap of ~3.2 eV, rendering it inactive under visible light. Approaches to optimize the TiO₂ photocatalyst, either by altering its morphological or chemical properties, have been conducted for many years, yet further modification of this semiconductor has the potential to yield photocatalysts with excellent properties and higher photocatalytic activity. This could be effectively explored using combinatorial synthesis coupled with high-throughput characterization approaches. Such an approach has been widely applied for the discovery of new functional materials, including photocatalysts. By using high-throughput synthesis and characterization technology, preparation and screening of materials on small sample scales can be accelerated; hence, new TiO₂-based photocatalysts with enhanced photocatalytic activity can be acquired more rapidly. Additionally, the large database of materials being systematically examined will greatly build our fundamental understanding of the relation between materials structure/composition and photocatalytic activity. This review details various high-throughput syntheses and characterization techniques applied to improve the photocatalytic properties of TiO₂ materials and discuss several challenges that have been raised or may be encountered in the future when using this approach.

KEYWORDS: high-throughput, combinatorial, TiO₂, photocatalysis, synthesis, characterization



1. INTRODUCTION

As a fundamental requirement for life, the availability of a clean environment cannot be understated. The negative effects of our lifestyle and continued industrial growth upon the environment, such as hazardous waste, water contamination and air pollution are inevitable. One approach to addressing this problem in part is photocatalysis that utilizes solar energy (which is abundant and clean) and has become an extremely active research area in recent years. Photocatalytic processes have been applied in various areas, such as water splitting to produce hydrogen,^{1–3} bactericides,⁴ self-cleaning materials,⁵ decomposition of crude spills,^{6–8} as well as in medical applications, such as inactivation of cancer cells.^{9,10} Semiconductors with photocatalytic properties are materials of choice due to their unique and beneficial characteristics. Titanium dioxide (TiO₂) in particular is widely studied for photocatalysis as it is nontoxic, abundant, inexpensive, and has tunable properties.^{11–13} A great number of reviews have been published covering various aspects of TiO₂-based materials for photocatalytic applications.^{11,12,14–17}

In most studies, the convention to produce and to assess the viability of a photocatalyst is by performing the synthesis and characterization one sample at a time, which can be time-consuming. Meanwhile, the challenge of developing new

photocatalysts and optimizing the photocatalytic activity of existing materials is quite demanding, requiring extensive workloads that are tedious, as they include the preparation of samples (often in gram quantity or slightly less) followed by laborious material screening. This is because the photocatalytic activity can be affected by many factors associated with the material properties and the testing conditions. To circumvent such time-consuming issues, researchers have changed the strategy of their research toward high-throughput methods. Here, the terms “combinatorial” and “high-throughput” are often interchangeably used to represent automated parallel or rapid sequential processing of either material synthesis or evaluation.¹⁸ The combinatorial synthesis and high-throughput screening method has been widely used since the late 1980s in pharmaceutical research to create new antibodies from a wide range of molecular libraries,^{19–21} as well as for new drug discovery.^{22,23} Such systems have then motivated researchers in the area of solid-state technology to create libraries of materials using a high-throughput approach. In 1995, the use of a combinatorial method to discover a new library of super-

Received: March 25, 2015

Revised: July 30, 2015

Published: September 15, 2015

conducting compounds was first demonstrated by Xiang et al.²⁴ This work caught the attention of researchers as it exhibited the potential of the high-throughput approach as an effective technique to create libraries of samples. Soon after, the high-throughput methodology, either in the form of synthesis or screening, was implemented for a wider range of applications, such as luminescence,^{25–27} magnetoresistivity,²⁸ ferroelectric/dielectric materials,²⁹ and solid-state catalysis.³⁰ In the field of photocatalysis itself, the high-throughput approach has been applied to either establish libraries of new photocatalysts or improve on existing materials. Figure 1 illustrates the number of

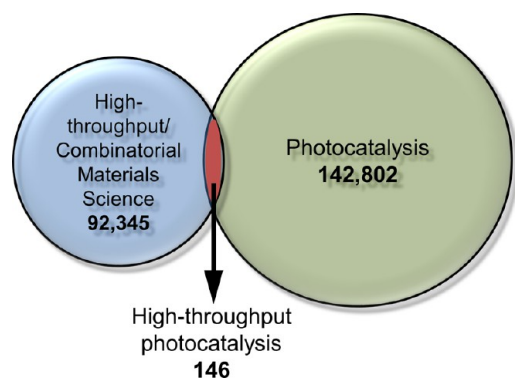


Figure 1. Comparison of the number of publications, including patents, appearing in the area of photocatalysis and high-throughput (within the scope of chemistry and materials science) with the intersect showing a relatively small number of publications combining both areas. Data was collected from Web of Science on March 20, 2015.

published manuscripts in the area of photocatalysis and high-throughput/combinatorial studies within the field of chemistry and materials science. High-throughput techniques have attracted much interest, but clearly this technique has had limited impact in the area of photocatalysis with just less than 150 papers published to date. This area of research holds great potential and, therefore, deserves an in-depth study.

A typical process cycle for the discovery of new materials using the high-throughput methodology is described in Figure 2a. As the focus here is high-throughput photocatalysis research, the processes are further detailed in Figure 2b. Initially, the material of interest should be defined and a group of related materials with certain variations should be determined. This step will be strongly affected by the main goal of the research itself. In principle, high-throughput studies are performed based on two different objectives: discovery of new materials and optimization of existing materials. The goal of the study will therefore affect the materials library design, however, the overall experimental procedure remains rather similar. The next step is material preparation, which can be categorized into two techniques, physical- or instrumental-based deposition and chemical-based synthesis. Following the synthesis step, the resulting material library is evaluated using high-throughput screening. The screening process for photocatalysts covers two aspects: material properties and photocatalytic activity, which could include several steps. First screening, for instance, could be done through a rapid process where hundreds of samples are tested. In this initial screening, the complexity of the tested parameter is kept low as the main purpose is to distinguish samples according to the main characteristic of interest. For practical reasons, to select lead

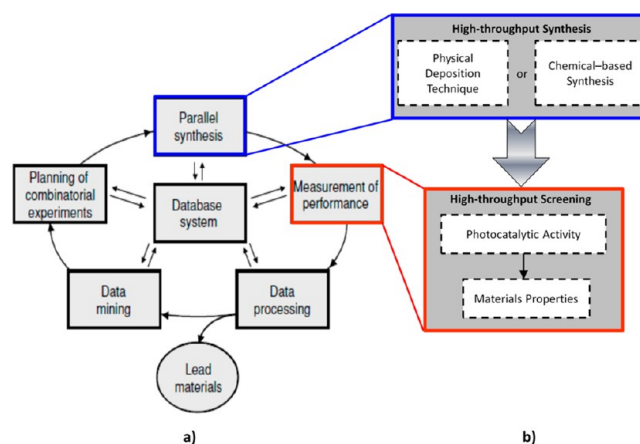


Figure 2. (a) Typical experimental procedure applied in combinatorial research in general, (b) high-throughput experimental flow including synthesis (blue box) and performance measurement/screening (red box) that are normally applied in photocatalysis research. Panel a is reprinted with permission from ref 33. Copyright 2005 IOP Publishing.

materials, most researchers assess the materials library based solely on the photocatalytic performance as their first screening step. Further screening tests can be conducted in order to identify the functional characteristics of the materials that correlate to the photocatalytic performance (either in high-throughput or, often, in low-throughput manner). It is essential when performing high-throughput screening to ensure that the analytical tool is valid. High-throughput screening is expected to be rapid as well as accurate; hence, a careful validation step prior to the experiments is a critical step that should not be abandoned so as to preserve the reliability of the results. Following analysis, the data is evaluated to either produce the final output or to be used for further feedback. Overall, the main advantage of the combinatorial research lies in the cycle model in which every processing step can be used to update the design of a material library database or be applied as a guide to improve future investigations in a rapid manner.^{18,31,32}

A number of reviews have been published covering high-throughput research with particular highlights on the discovery of new materials,^{18,34} including catalysts, solid state materials,^{35,36} and thin films.^{37–40} These reviews signify the emerging development of high-throughput research over the past few years. However, to the best of our knowledge, there has been little published in the area of photocatalysis to date. Gao and his group provided a review on the development of high-throughput synthesis and screening in photocatalyst discovery in general.³² Here, we specifically aim to review the implementation of high-throughput techniques for the development of TiO₂ photocatalyst materials. Particular emphasis has been placed on TiO₂ as this material has been the most widely studied and applied in the area of photocatalysis due to its excellent photocatalytic activity, abundance, nontoxicity, and stability.^{11,12} The basic mechanism of photocatalysis and its related theories will be summarized first. Then, a comprehensive review on the recent progress of high-throughput methodologies for photocatalysis applications will be presented. This discussion comprises two sections: the combinatorial approach for the synthesis of TiO₂ materials and the characterization techniques. Although the primary focus is on TiO₂, some of the discussions on the high-throughput approach also include other materials. This is required to provide further

insights, as well as to demonstrate the potential application of combinatorial approaches to TiO₂ materials research. To conclude, a brief overview of the progress made so far in combinatorial research of titania-based photocatalysts and its future prospect toward further development is presented.

2. FUNDAMENTALS OF PHOTOCATALYSIS

2.1. Basic Principles. *Photocatalysis* is a term used to define a process in which light changes the rate of chemical reaction in the presence of a substance that absorbs the light. This light-absorbing substance is referred to as the *photocatalyst*. A great interest in the study of photocatalysis emerged after the early 1970s when the photocatalytic splitting of water into O₂ and H₂ using TiO₂ and Pt electrodes in a photoelectrochemical system was reported by Fujishima and Honda.⁴¹ There has been a sharp increase in the number of published papers produced by various researchers devoted to photocatalysis in the past two decades.⁴² In general, these studies focused on three areas: to obtain an understanding of the fundamental photocatalytic mechanism, to enhance the photocatalytic activity of photocatalysts, or to improve the photocatalytic efficiency by modifying the photocatalysis reactor set up.

Photocatalytic reactions may occur either homogeneously or heterogeneously.^{11,43,44} In homogeneous photocatalysis, the catalyst and the reactants are in the same phase. For example, the ozonation of water to degrade organic materials, where ozone acts as a direct photocatalyst that is dissociated upon UV illumination and produces $\cdot\text{OH}$ radicals after reacting with water.^{45,46} In heterogeneous photocatalysis, the reactants and catalyst exist in different phases. The reaction system generally involves a solid photocatalyst (in the form of metal oxides or semiconductor, e.g., TiO₂) that is in contact with either a liquid or gas phase containing the reactants.

Photocatalysis involves a photoexcitation mechanism that can be classified into two different types: “catalyzed photoreaction” and “sensitized photoreaction”.¹² In a catalyzed photoreaction, photoexcitation occurs in the adsorbate molecules that then interact with the ground state catalyst substrate. If the initial photoexcitation occurs in the catalyst substrate followed by transfer into ground state molecules this is referred to as a sensitized photoreaction. Here, the discussion will focus on the sensitized photoreaction rather than catalyzed photoreaction as the sensitized photoreaction is mostly found in semiconductor-based heterogeneous photocatalysts.^{12,47}

Semiconductors are the most common materials used in heterogeneous photocatalysis because of their unique properties. Furthermore, their solid form facilitates high stability and mobility of charge for interaction with the adsorbate molecules in the surrounding medium.^{11,12} A semiconductor, by definition, is a material with medium conductivity, which is below the conductivity of conductors (metals) and above insulators. The conductivity of semiconductor materials can be explained by their electronic structure, which is characterized by a filled valence band and an empty conduction band. An empty energy region, where no energy levels exist, extends between these two energy bands and is referred to as the *bandgap energy* (E_g). In general, the critical mechanism of semiconductor-mediated photocatalysis consists of two primary steps: the photon absorption and charge transfer process. Initially, the absorption of a photon with energy greater than the E_g of the semiconductor will generate an electron–hole pair within the conduction band (CB) and valence band (VB), respectively. The photoexcited electron–hole pairs undergo one of two

subsequent charge transfer paths (Figure 3): (1) recombine with each other and dissipate heat (path a) or (2) migrate to

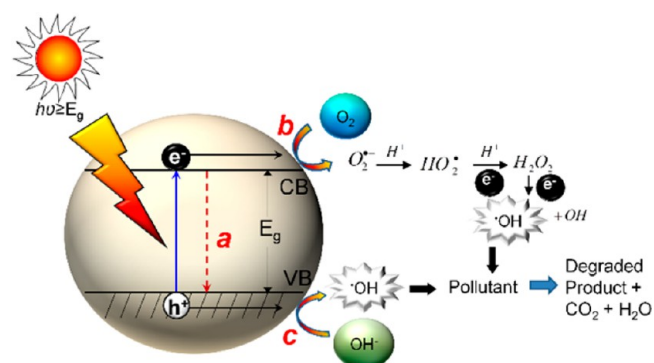
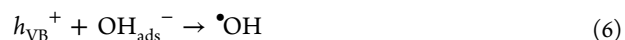
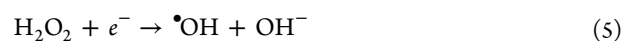
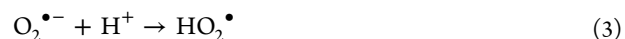
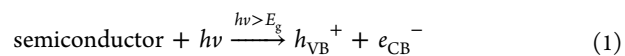


Figure 3. Schematic diagram of photoassisted charge transfer in a semiconductor during the photocatalysis process that include either recombination (a) or electron (b) and hole (c) migration to the semiconductor surface, followed by redox reaction with the adsorbates.

the semiconductor catalyst surface and induce redox reactions with the adsorbates (paths b and c). The first pathway, which is recombination, could occur either at the surface or within the bulk of the semiconductor because of crystal imperfections, such as defects or the presence of impurities.⁴⁸ Meanwhile, the second pathway leads to separate reactions for the electrons and holes. Electrons contribute to a reduction reaction with an acceptor—usually oxygen (path b), whereas holes may combine with electrons from the donors (path c). An example of the overall reaction in semiconductor photocatalysis is summarized in eqs 1–6.¹¹ Photoexcited electrons (e_{CB}^-) react with oxygen to generate superoxide radicals ($\cdot\text{O}_2^-$) that will undergo subsequent reactions to produce hydroxyl ($\cdot\text{OH}$) radicals. Meanwhile, holes in the valence band (h_{VB}^+) react with the surface hydroxyl group or adsorbed water to form $\cdot\text{OH}$ radicals. These radical species then react with adsorbed or closely associated organic molecules and eventually oxidize them into CO₂ and H₂O (and HCl if chlorine forms part of the organic molecule).¹¹ In addition to these reactions, Teoh et al. provide a summary of other reactions that could also occur following photoexcitation within a semiconductor, resulting in electron and hole pairs.⁴² For heterogeneous catalysis using a TiO₂ catalyst, more detailed interfacial charge-transfer mechanisms and reactions, including characteristic times for each step, can be found in a number of reviews.^{11,49–51}



Quantum yield is generally the parameter used to measure the efficiency of photocatalytic activities within a system. The quantum yield (Φ) is defined as the ratio of the number of molecules converted (i.e., mol of the reactant consumed or product formed) to the number of photons absorbed.⁵² In

practice, the actual light absorption is difficult to quantify due to photon scattering at the semiconductor surface and transmission through the semiconductor. Therefore, the term “apparent” quantum yield (Φ_{app}), which is defined as the ratio between reaction rate and incident light intensity (I_a) has often been used instead.⁴⁷ The mathematical expression of apparent quantum yield is given in eq 7, where n is the number of molecules that react at a certain time t , and I_a is the quantity of absorbed photon flux from monochromatic light during the same time. For the case where polychromatic light is used, I_a should be replaced by I , which represents the total incident light intensity. The resulting quantum yield is often referred to as the formal quantum efficiency (FQE), which is generally less than Φ_{app} .⁴⁷ The rate of reaction (dn/dt) is strongly affected by the rate of the charge transfer processes, k_{CT} , and inversely proportional to the rate of recombination, k_{R} eq 8.¹² This mathematical formula highlights that recombination is a limiting process in photocatalytic reactions and therefore should be minimized. Recombination is detrimental as it will reduce the population of highly charged electrons and holes for further redox reactions.

$$\Phi_{\text{app}} = \frac{dn/dt}{I_a} \quad (7)$$

$$dn/dt \propto \frac{k_{\text{CT}}}{k_{\text{CT}} + k_{\text{R}}} \quad (8)$$

To determine the apparent quantum yield, illumination intensity is one of the important factors that affect the photocatalytic degradation rate.⁵³ This is because the photo-generated electron–hole pair population is proportional to the number of photons absorbed, which therefore affects the number of hydroxyl radicals and reactive oxygen species on the semiconductor surface. The relationship between light intensity and photodegradation reaction rate has been controversial. While some argued that photodegradation is significantly enhanced in the presence of high intensity photons,⁵⁴ others reported that the relationship varies depending on the intensity of the given light.^{55,56} The other important factors affecting the photocatalytic reaction rate are light distribution within the reactor,⁵⁷ catalyst concentration,⁵⁸ solution pH,^{59,60} concentration of both catalyst and contaminant,⁶¹ temperature,⁶² and the addition of dissolved oxygen.⁶³ Further details on the influence of these factors can be found in several reviews.^{53,64,65}

2.2. Charge Transfer Physics in Semiconductors. To improve the photocatalytic activity of any particular semiconducting material, it is imperative to understand the fundamental physics of the system, including the kinetics of semiconductor–liquid or –gas phase contacts. The mechanism of the charge transfers on the semiconductor interface (e.g., semiconductor–metal/liquid/gas) is mainly determined by the difference in electron affinity or electrochemical potential between two materials. This implies the likelihood of these materials to either lose or gain electrons. An electric field is consequently produced by the interface of two materials and is generally formed within 5–200 nm from the semiconductor surface, whereas the direction is determined by the relative electron affinity of both phases.⁶⁶ For example, n-type semiconductors (a semiconductor that contains excess electrons) can have surface states that act to trap electrons and cause the surface to become negatively charged. This will attract holes toward the surface and repel electrons toward the

semiconductor bulk; hence causing a bending of band edges upward toward the surface and the generated electric field will result in electron–hole separation (see Figure 4).

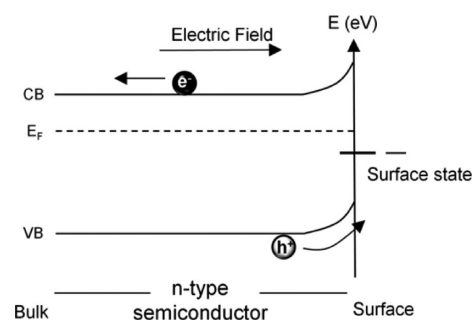


Figure 4. Electric field formation and charge separation within the semiconductor surface due to negatively charged surface state.

A similar mechanism also applies in the presence of semiconductor–solution/gas phase contact, which is typically found in semiconductor powder-based photocatalysts or photoelectrochemical cells. Figure 5 depicts the space charge

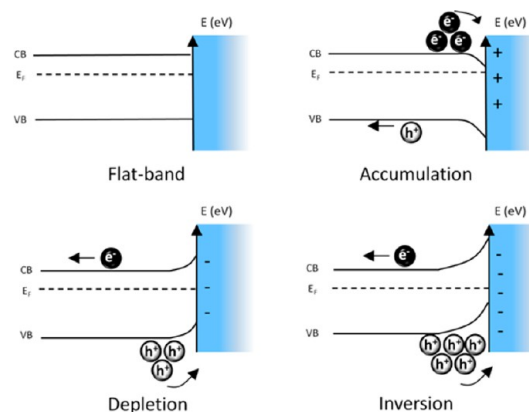


Figure 5. Formation of a space charge layer and band bending at an n-type semiconductor surface under different conditions depending on the presence of charge at the semiconductor–liquid interface.

layers formed across the interface of an n-type semiconductor upon contact with solutions containing different charges. A flat-band refers to a condition in which there is no space charge region present before any contact occurs. The formation of a space charge region following subsequent contact with the electrolyte solution can be classified into three different cases. When the solution contains positive charges or acceptor species, electrons as the majority carrier in an n-type semiconductor are attracted toward the surface; hence, their surface concentration is significantly increased and the surface band edge bends downward, with the conduction band approaching the Fermi level. This condition is referred to as accumulation. In contrast, when the solution contains negative charges or dopant species, the surface concentration of holes as the minority carrier increases owing to charge neutrality and the bands bend upward. The space charge layer formed under this condition is called the depletion layer. If the concentration of dopant species within the solution is increased, the surface band energy bends further upward, with the valence band edge approaching the Fermi level. This condition forms a space charge region called an inversion layer. Under inversion

conditions, the n-type semiconductor surface appears as an imaginary p-type semiconductor because of the high concentration of holes near the surface.

After understanding the charge transport within the semiconductor surface and bulk with respect to the presence of charge across the interface, it is also essential to comprehend the concept of redox reactions with the adsorbate molecules. The rate and probability of the redox reactions occurring at the semiconductor–solution interface are determined by the band edge position of the semiconductor in correlation to the redox potential of the adsorbate materials.¹² Therefore, one of the critical factors influencing the efficacy of semiconductor photocatalysts in degrading organic compounds is their bandgap edge positions. The lower-edge position of the conduction band can be used to measure the reduction strength of the photoexcited electrons, whereas the upper-edge position of the valence band can be considered to measure the oxidation probability of the photoexcited holes. The redox potential of the $\text{H}_2\text{O}/\cdot\text{OH}$ is generally required to be within the semiconductor bandgap.⁶⁷ Figure 6 shows the band edge

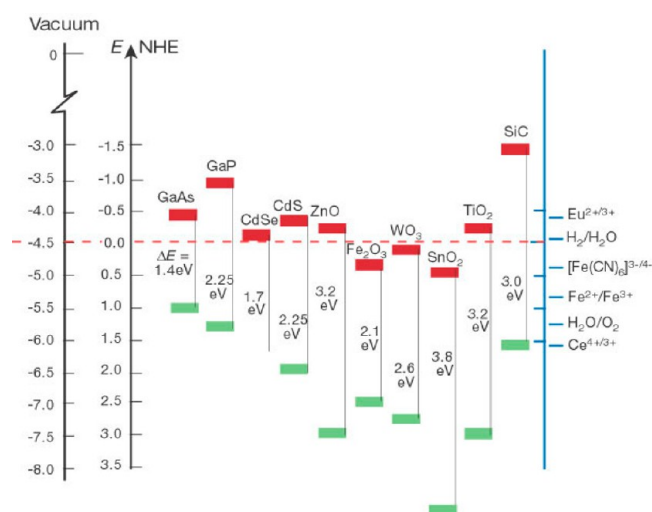


Figure 6. Energy level diagram indicating conduction (red) and valence (green) band edge positions for various semiconductors in contact with an aqueous electrolyte at pH = 1. The energy scales are in electron volts using either a normal hydrogen electrode (NHE) or vacuum energy level as the reference. Reprinted with permission from ref 68. Copyright 2001 Macmillan Publishers Ltd.: Nature.

energy levels of several semiconductors in an aqueous solution of pH 1 with respect to the redox potentials of hydrogen ($\text{H}_2/\text{H}_2\text{O}$), oxygen ($\text{O}_2/\text{H}_2\text{O}$), and several other elements.⁶⁸ For water splitting, SiC, TiO_2 , ZnO, CdS, and CdSe would be excellent materials as their oxidation and reduction power is strong enough to enable the production of hydrogen and oxygen. However, this does not necessarily preclude the rest of the materials as suitable photocatalysts. There are several ways to improve their photoactivity, for instance with the addition of, or combination with, other materials, details for which are given later.

3. TiO_2 PHOTOCATALYSTS

Titanium dioxide (TiO_2) is typically considered as an n-type semiconductor as the result of oxygen vacancies and Ti interstitials that act as donor type defect.⁶⁹ There are three different TiO_2 polymorphs, that is, anatase, rutile, and brookite.

Unlike brookite, which is generally difficult to prepare, anatase and rutile have been preferred in many photocatalytic studies.¹⁴ Additionally, these polymorphs display differing photocatalytic activities owing to their different crystal structures as characterized by their lattice and electronic band structures. The bandgap energy for anatase and rutile is 3.2 and 3.0 eV, respectively.^{70,71} Although anatase is metastable and rutile is the most stable form of TiO_2 , anatase has been widely reported to give the best photocatalytic activity and photostability.⁷² Its slightly higher Fermi level (0.1 eV) over that of rutile, which leads to lower oxygen affinity and a higher number of surface hydroxyl groups are believed to give the improved performance.¹⁴ Also, the relatively high intrinsic radiative recombination observed within rutile TiO_2 nanoparticles, as observed from photoluminescence studies, is suspected to further limit its use as an active photocatalyst.⁷³

To select semiconductor photocatalyst materials, several factors need to be considered including the stability of the semiconductor under illumination, the wavelength response, and the efficiency of the photocatalytic process. As previously discussed in relation to Figure 6, some materials could be considered as photocatalysts based on their bandgap energy, however, not all of them would meet the aforementioned criteria. For example, CdS with a bandgap energy of 2.42 eV may have band edges in suitable locations for redox reactions and high absorption in the visible light spectrum, but it photodegrades with time.⁷⁴ Contrarily, TiO_2 is relatively stable but is only active in the UV range ($\lambda < 400$ nm), exhibiting poor visible light response due to its higher bandgap energy. This is a major constraint as the solar spectrum only consists of approximately 4–5% of UV light.⁷⁵ However, TiO_2 , as a photocatalyst, remains favored due to its low cost, stability, abundant availability, and tailorable electronics properties and morphology. In an attempt to overcome its limitation, many experiments have been conducted to modify the surface or bulk properties of TiO_2 . The challenge in improving the photocatalytic activity of TiO_2 , in general, revolves around two main issues: to acquire optimum photocatalytic reactions and to increase the population of charge carriers. The rate of photocatalytic reaction can be enhanced by preparing materials with high active surface area. Meanwhile, a high population of photogenerated electron–hole pairs can be obtained either by increasing light absorption from a wide range of the light spectrum or by limiting the rate of electron–hole recombination. Strategies to achieve all of the above improvements can be grouped into two approaches as discussed in sections 3.1 and 3.2.

3.1. Morphological Modification. The aim of this modification is to increase the surface area by either creating smaller crystals or adding porosity. A smaller crystallite size and highly porous structures provide a high surface to volume ratio, thereby increasing the likelihood of adsorption of the organic pollutant, increasing the photocatalytic reaction centers, and also decreasing bulk recombination.⁷⁶ The sol–gel method has been the most widely reported technique applied to produce such structures because it is facile yet allows relatively fine control over the morphology and porosity of the material. Monodisperse TiO_2 nanoparticles have been the most popular form studied to date due to the ease in controlling the diameter and porosity of the particles.⁷⁷ Meanwhile, research on the synthesis of porous TiO_2 has emerged in the last few decades with mesoporous structures (pore diameter 2–50 nm) being the most studied among others.⁷⁸ Common synthesis

techniques used to prepare ordered mesoporous TiO₂ materials usually include sol–gel synthesis combined with soft templating,⁷⁹ hard templating,⁸⁰ and template-free methods.⁸¹ As a result of the various modifications, different forms of titania nanostructures that include porous beads,⁸² hollow spheres,⁸³ nanotubes,⁸⁴ nanowires,⁸⁵ nanorods,⁸⁶ nanofibers,⁸⁷ and nanoribbons,⁸⁸ have been reported. Scanning electron microscopy images of some of these morphologies are shown in Figure 7. Excellent reviews on the synthesis and general applications of mesoporous TiO₂ materials can be found in the literature.^{17,89}

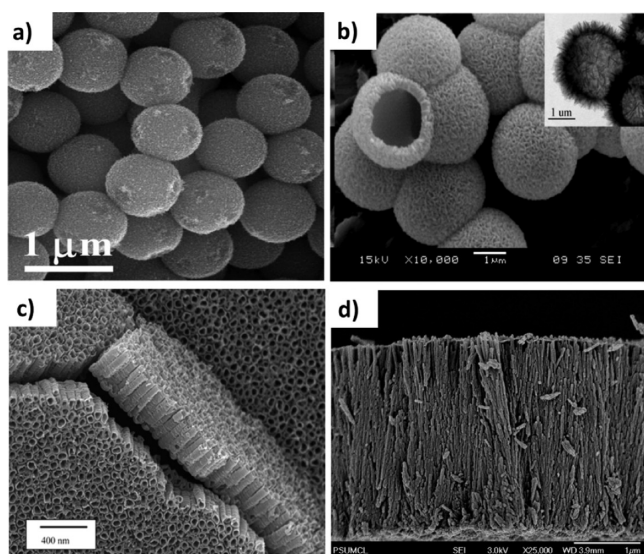


Figure 7. SEM images of TiO₂ with various morphologies: (a) spheres,⁸² (b) hollow spheres,⁸³ (c) nanotubes,⁸⁴ and (d) nanowires.⁸⁵ Reprinted and adapted with permission from ref 82, Copyright 2010 American Chemical Society; ref 83, Copyright 2007 American Chemical Society; ref 84, Copyright 2006 American Chemical Society; and ref 85, Copyright 2008 American Chemical Society.

3.2. Modification of Electronic Properties. This approach is performed primarily to increase the population of electron–hole carriers by modifying the intrinsic properties of the photocatalysts. Modification of either the surface properties or bulk properties of TiO₂ can be achieved in several ways: (i) prolonging the lifetime of charge carriers, (ii) introducing new energy states within the bandgap, or (iii) narrowing the bandgap by shifting the conduction band or valence band to allow photoexcitation at lower energy.

These modifications are usually obtained through the incorporation of additional elements into the TiO₂ network, such as doping with metal or nonmetal elements, coupling with another semiconductor, or sensitizing the TiO₂ surface. Much research has been conducted in this area, as highlighted in this section with the corresponding mechanisms described in Figure 8.

The incorporation of metal elements into TiO₂ has been the most widely reported approach to suppress electron–hole recombination. This may include doping into the TiO₂ lattice or modifying the surface by embedding metal nanoparticles. Modification of the TiO₂ bandgap by doping with metal, transition metal, and rare-earth metal ions has improved the photocatalytic activity of TiO₂ by creating an energy level between the conduction and valence band because of the presence of impurity (Figure 8a). This modification shifted the

spectral response of TiO₂ toward the visible light region, thus positively affecting the photocatalytic activity.⁹⁰ Regardless of the type of metal ions chosen, the challenge remains in determining the optimum level of metal in the sample as quantities above the optimum become detrimental. Transition metal ion doping was also reported to cause thermal instability in anatase.⁴⁸ Importantly, the resulting photocatalytic activity of the metal ion doped-TiO₂ is determined by the preparation method. There have been various attempts to incorporate metal into TiO₂ using either chemical doping (impregnation method)⁹¹ or physical deposition such as the ion implantation technique.⁹² Some authors argued that the impregnation method may have limited impact as it only generates substitution of the metal ions onto TiO₂ surfaces and hardly into bulk TiO₂ lattices. In contrast, the latter method has been shown to create bandgap narrowing of TiO₂, resulting in the successful substitution of Ti ions within the TiO₂ lattices with the implanted metal ions (see Figure 8a).^{90,93}

The addition of noble metal nanoparticles such as Ag, Au, Pt, and Pd have also been intensively investigated and shown to be very effective in enhancing the photocatalytic activity of TiO₂ with the optimum metal concentration depending on the metal type.⁹⁴ The reason for this improved photocatalytic performance is due to the higher work function of the noble metals, when compared with that of TiO₂, enabling them to act as effective electron sinks that attract photoexcited electrons from the conduction band of TiO₂.

Another successful approach in modifying TiO₂ properties is to introduce nonmetal elements. This is an attractive option because of lower materials cost compared with the cost of metal doping. Nitrogen has been the most widely studied nonmetal dopant because of its comparable atomic size with oxygen, small ionization energy and high stability, allowing it to be easily introduced into the TiO₂ as a substitution element in the oxygen lattice sites or the interstitial lattice sites.⁹⁵ Through a similar mechanism, the addition of carbon, phosphorus, and sulfur have also lead to positive photocatalytic improvements under visible light irradiation through lattice parameter modification resulting in bandgap narrowing,^{96–98} although S-doped TiO₂ is rather difficult to prepare compared to N-doped TiO₂. Fluoride doping into TiO₂ has shown positive enhancements via a different mechanism. The incorporation of F[−] induces partial conversion of Ti⁴⁺ to Ti³⁺ via charge compensation, thereby improving charge separation as Ti³⁺ can act as an electron trap.⁹⁹ Other promising approaches include nonmetal codoping, for example, N–F-co-doped TiO₂,¹⁰⁰ and the synthesis of oxygen rich TiO₂ structures.¹⁰¹

Coupling with a different semiconductor has been another option to improve the photocatalytic efficiency of TiO₂ by harnessing the advantages of the individual semiconductors and overcoming their respective limitations. For example, coupling TiO₂ with a semiconductor possessing a suitable bandgap for visible light absorption, such as CdS ($E_g = 2.4$ eV), despite CdS being less stable, improves the spectral response of TiO₂ as the main photocatalyst. Thus, the overall photocatalytic efficiency of the coupled system in the visible light range is improved due to electron transfer from CdS to TiO₂ following absorption of visible light by CdS, effecting charge separation (see Figure 8b).¹² However, one should note that the electron transfer in this approach can only occur if the conduction band of the coupled semiconductor is higher than the conduction band of TiO₂. Therefore, the bandgap properties of the selected semiconductor must be considered. Carbon nanotube

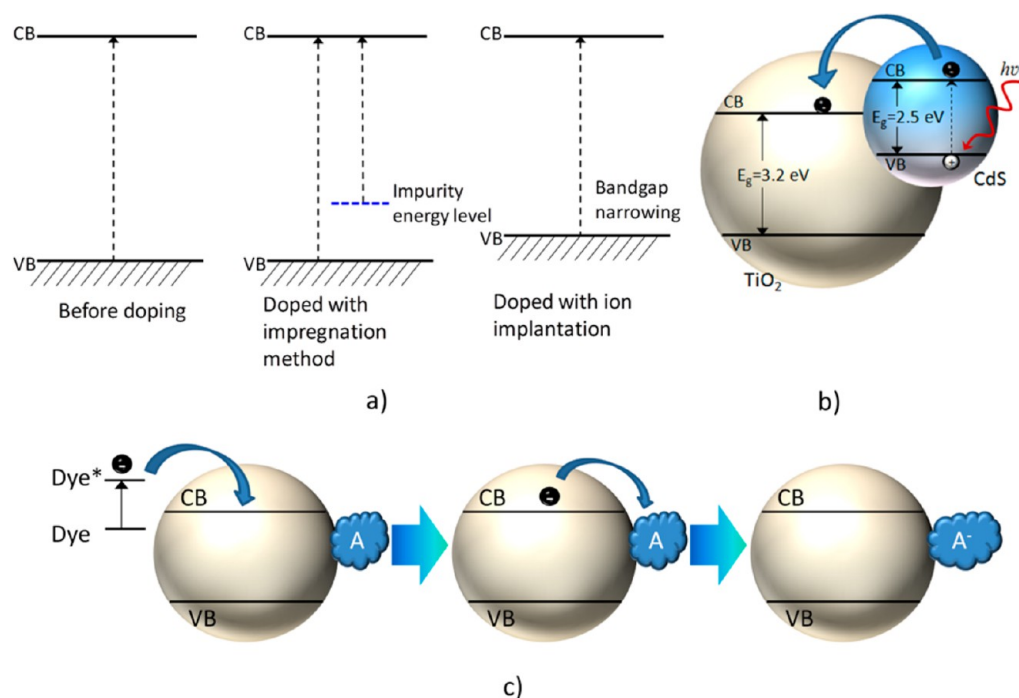


Figure 8. Proposed energy level configurations in modified-TiO₂ semiconductors leading to improved photocatalytic activities: (a) band structure before and after bulk modification via doping, which could introduce a new energy level and bandgap narrowing, (b) enhanced photoexcitation via coupling with CdS, and (c) multiple electron excitation steps, using a dye sensitizer, which involve electron transfer from the dye to the conduction band of the TiO₂ then into an adsorbed organic acceptor molecule (A).

(CNT)-TiO₂ composites have also shown improved photocatalytic activities compared to that of titania due to prolonged carrier lifetime and higher surface areas, leading to more OH radical formation.¹⁰² As an alternative approach to improve the spectral response of the photocatalyst, surface sensitizing is effective as it provides additional electrons from the photoexcited dye molecules, as illustrated in Figure 8c. This principle has been widely applied in photovoltaic applications (dye-sensitized solar cells).¹⁰³

The above modifications give a large number of choices in regards to the synthesis of TiO₂ materials with varied configurations and structures and/or their combination with other materials or dopants, either as single or multiple elements (i.e., codoping). As such, considerable effort is required to search for the optimal material combination giving the highest photocatalytic efficiency. Therefore, the use of high-throughput methods is an effective approach giving rapid preparation and quick screening of numerous materials, which will be discussed in the next sections.

4. HIGH-THROUGHPUT MATERIAL PREPARATION

The combinatorial approach has been developed to allow synthesis of a large number of materials in an efficient manner. Determination of the rapid synthesis method used in combinatorial experiments is affected by the form of the chosen material. For TiO₂, combinatorial synthesis is generally used to produce either powders or thin films. In addition, parameters related to the preparation method, as well as the compatibility of the high-throughput analytical techniques that will be carried out afterward need to be considered. Reviews on high-throughput material synthesis have been reported by several groups for materials with a range of applications, for example for solar water splitting,¹⁰⁴ electronics, catalysts and polymers,^{18,34,35} and also nanotechnology research.¹⁰⁵ This

section focuses on several synthesis techniques applied for the combinatorial production of TiO₂-related photocatalyst materials, both in the form of powders and thin films.

4.1. Synthesis of Powders. The sol-gel chemistry method has been the most common approach used to synthesize libraries of photocatalyst powders. This method in principle offers some advantages, such as ease of processing, fine-tuning of materials properties, homogeneity, and flexibility in material compositions, including the introduction of dopants, all of which can be controlled through the synthesis conditions. In the case of high-throughput screening, it is worth mentioning that the use of sol-gel chemistry to prepare the material libraries containing large numbers of samples is the most widely reported.^{106–109} In a high-throughput sol-gel synthesis, a library of materials is usually synthesized by a robotic apparatus producing small quantities of sample for each variation within small vials (typically with 2 mL capacity), which also serve as microreactors, and then rapidly screened to obtain the optimum material. This method was first reported by Lettmann et al., who created libraries of oxide-based materials containing 45 samples each.¹¹⁰ These oxide-based materials were screened and tested as potential photocatalysts using a TiO₂-based library as a reference. The synthesis process was performed within high performance liquid chromatography (HPLC) flasks, using a robotic apparatus (*Tecan Miniprep 50*), to facilitate further screening using HPLC. For TiO₂ and SnO₂ libraries, tetraisopropoxides were used as the metal oxide precursors, and Na₂WO₄ was used to synthesize the WO₃-based materials. Hydrochloric and nitric acids (when Pb or Ag dopants were involved) were added to accelerate the gelation. An orbital shaker was employed throughout the preparation process to aid the mixing of reagents. After gels were formed, all of the libraries were aged for 2 weeks, calcined at 400 °C for 3 h and then underwent screening. A similar automated procedure

was also reported by Seyler et al. to prepare various doped titanium oxides in 2 mL gas chromatography (GC) vials placed in a 5×10 rack.¹¹¹ The modified sol-gel reaction was controlled using *Plattenbau* software and the synthesis was performed by a commercial pipetting robot. All samples were mixed using an orbital shaker then aged for 3 days and calcined at 720 °C according to a specific ramp program.

The synthesis of TiO₂ nanoparticles has also been reported using a continuous hydrothermal flow synthesis (CHFS). The basic principle of this system is to mix a stream of superheated water with a metal ion stream in solution, which subsequently produces precipitation of the metal ions as nanoparticles because of the rapid change in their environment.^{112–114} The schematic of this system is shown in Figure 9.¹¹² For

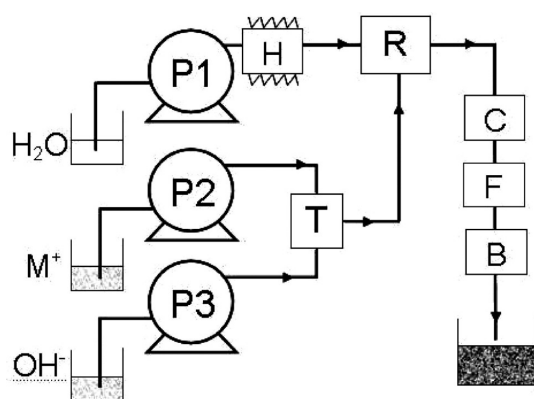


Figure 9. Schematic configuration of a continuous hydrothermal flow synthesis system for producing TiO₂ nanoparticles doped with various metal ions (M = metal ion, P = pump, T = T-piece mixer, H = heater, R = counter current reactor, C = cooling, F = filter, and B = back-pressure regulator).¹¹² Reprinted with permission from ref 112. Copyright 2007 American Chemical Society.

photocatalysis, Thompson et al. reported the use of CHFS to produce TiO₂ nanopowders doped with Zn²⁺, Sr²⁺, La³⁺, Ag⁺, and Pr³⁺.¹¹⁵ Titanium(IV) bis(ammonium lactato)dihydroxide (TiBALD) was used as the main reagent. The reaction processes of the reported CHFS system are as follows: first, metal salt dopants were added to a diluted TiBALD solution (0.4 mol/L). The metal salt solution from pump 2 was subsequently combined with water from pump 3 in a T-piece mixer. This mixture was then brought into contact with preheated water at a supercritical temperature of 400 °C and pressure of 24.1 MPa in a counter current mixer, in which a stream of nanoparticles was subsequently generated. The nanoparticles were then cooled, collected, and centrifuged. Following the removal of the supernatant, samples were subsequently washed in ethanol, recentrifuged, washed in DI water twice, and then freeze-dried for further characterization. The CHFS route showed potential in producing a large number of metal doped compounds in a relatively short time.

In addition to sol-gel chemistry and CHFS, combustion synthesis has been employed to produce catalyst powders in a parallel manner. The solution combustion technique involves rapid heating of a solution, inducing the instantaneous formation of crystalline materials at high temperatures (up to 800 °C) within a short time. The application of a single-step solution combustion method has been reported by some authors; for example, Nagaveni et al. used this method to produce metal doped TiO₂ photocatalyst powders.^{116–118} Gao

et al. also demonstrated that solution combustion is applicable for combinatorial production of luminescent materials libraries in the form of powders under high synthesis temperature.¹¹⁹ They have successfully fabricated a combination of mask and microreactor array made from a corundum substrate to facilitate parallel reactions. Masks and copper nets were employed to contain the synthesized powders in their individual microreactors. A similar setup was also used to synthesize and assess a new class of photocatalysts based on ABO₃ binary oxides (A = Y, La, Nd, Sm, Eu, Gd, Dy, Yb; B = Al, In), which are active under visible light.¹²⁰ Another technique that can potentially be applied for high-throughput material preparation is gas phase flame synthesis. Dhupal et al. reported the application of this method to synthesize titanium suboxide nanoparticles (TiO_x with $x < 2$), that are photocatalytically active under visible light.¹²¹ The high temperature of the flame aerosol reactor breaks the Ti–O bonds and the oxygen can be subsequently removed from the lattice. The degree of oxygen deficiency can be subsequently manipulated by controlling the oxygen flow and flame temperature, making this system an attractive one-step high-throughput synthesis method for nanostructured materials preparation.

As another alternative method, Gao's group reported the use of a homemade drop-on demand inkjet delivery system to prepare nanoparticle suspensions of insoluble rare earth oxides in pure water to produce photoluminescent materials.¹²² Their setup consisted of computer-operated piezoelectric inkjet heads with each head connected to a suspension reservoir. The microreactor ceramic wells were fixed beneath the dispenser head. This method is particularly suited to highly stable (nonagglomerated) insoluble precursor suspensions with low viscosity. Thus, the implementation of this method toward the synthesis of TiO₂, which has not been reported, is worth investigating since the preparation methods commonly use liquid precursors or solution routes.

4.2. Thin Film Deposition. The preparation of thin film materials using combinatorial techniques has been more frequently reported than powder synthesis. This is partly due to the fact that films can be simultaneously synthesized in large batches; hence, providing more feasibility for high-throughput approaches. It is also synthetically versatile as it has the advantage of forming artificial lattices, epitaxial overlayers, and patterned films over a significant range of materials.²⁴ Reviews of thin film synthesis and the deposition of various functional materials for different applications (mainly for catalysis), using the high-throughput approach can be found in several references.^{34,35,38,39} The high-throughput deposition techniques vary, including electrochemical deposition,³¹ sputtering,²⁴ molecular beam epitaxy,¹²³ chemical vapor deposition,¹²⁴ physical vapor deposition,¹²⁵ metal organic decomposition,¹²⁶ and inkjet printing technology.¹²⁷

Sputtering techniques, using either radio frequency (RF) or direct current (DC), have been employed to produce TiO₂ films for over a decade.^{128–130} This method was also the first reported in combinatorial catalyst discovery in which a suitable physical masking technology was employed to isolate samples with diverse parameters. In 1995, Xiang et al. developed the first application of parallel RF magnetron sputtering to deposit arrays of superconducting copper oxide thin films using physical masks.²⁴ The library was synthesized by sputtering the precursors through a series of binary masks made by overlaying a primary mask with a series of secondary masks. Then, the thin films were sintered at 840 °C. Masking could be

performed using either physical shadow masks or photolithographic lift off.³⁵ The number of compounds that can be synthesized at the same time using these techniques was limited by the spatial resolution of the mask, thus high resolution physical masks are an essential requirement for a high density library, as well as high resolution scanning detectors to analyze the library. An efficient masking technology was also critical for the application of other techniques such as combinatorial laser molecular beam epitaxy (CLMBE), a combination of laser MBE and combinatorial masking system. Koinuma's group applied CLMBE to deposit artificial lattices and heterojunctions with control of the composition, thickness, and sequence in each layer at atomic scale.^{131–136} In addition to the masking, their distinct innovation included an in situ monitoring system called reflection high energy electron diffraction (RHEED), which was applied to monitor the growth of the deposited films.¹³⁴ The conceptual schematic configuration of CLMBE featuring RHEED is shown in Figure 10. Matsumoto et al. have

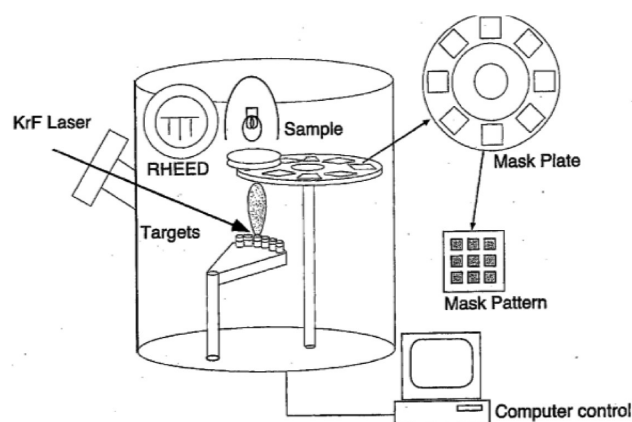


Figure 10. Schematic configuration of combinatorial laser beam molecular beam epitaxy (CLMBE) combined with reflection high energy electron diffraction (RHEED) to monitor the in situ reaction. Multiple target pellets can be used in this configuration and various moving mask plates can be placed between the heated sample and target to allow deposition of single, binary or ternary thin films. Reprinted with permission from ref 135. Copyright 2000 SPIE.

demonstrated the application of such systems to obtain anatase and rutile TiO_2 films doped with transition metals grown on SrTiO_3 and Al_2O_3 , respectively.¹³⁵ By using pulsed laser deposition (PLD) of target oxides, Koinuma et al. also reported the fabrication of TiO_2 films with varying thickness, ranging from 0 to 40 nm on a conductive Nb-doped TiO_2 substrate.¹³⁶ The film was subsequently immersed in AgNO_3 solution under UV irradiation. The resulting Ag precipitation was then characterized using an X-ray fluorescence technique to analyze the degree of photocatalytic activity across the film. The highest photocatalytic activity was achieved with TiO_2 films with a thickness of ~ 5 nm. They additionally demonstrated a new design of combinatorial autoclave reactor for probing novel catalysts via CO_2 copolymerization.

Chemical vapor deposition (CVD) has been frequently used to synthesize various types of thin films, including TiO_2 , for both research as well as industrial applications. It is a versatile technique that can be employed to coat a large surface area in a relatively short time. The application of combinatorial atmospheric pressure CVD (c-APCVD) to deposit a large area TiO_2 film has been demonstrated by Parkin's

group.^{124,137,138} One of their studies reported the preparation of a nitrogen doped TiO_2 film with gradual nitrogen composition and tunable crystal phase from anatase to an anatase–rutile mixture.¹²⁴ The film was deposited on a glass substrate coated with SiO_2 as a barrier layer. The precursors employed were TiCl_4 and ethyl acetate (as the oxygen source), which were heated and transferred by N_2 as the carrier gas into one chamber for mixing. Ammonia and plain N_2 were then flowed separately into the reactor to react with this mixture. As the oxygen from the ethyl acetate and nitrogen entered the reactor, a gradient of O:N ratios were formed across the film. This subsequently produced N-doped TiO_2 films with gradation of color, whereby the intensity of the yellow tint was proportional to the nitrogen concentration. The resulting film was divided into 247 regions according to variation in composition, and characterized for crystallinity, thickness, and N:Ti ratio using various analytical tools. A similar method has also been demonstrated to create continuous TiO_2 thin films doped with varying amounts of tungsten (see Figure 11a).¹³⁹

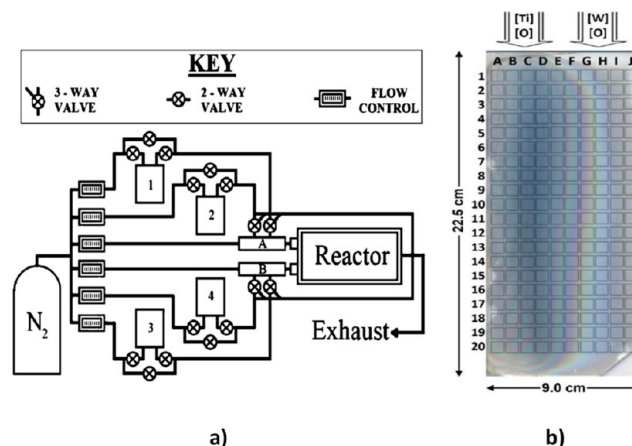


Figure 11. (a) Schematic diagram of the combinatorial atmospheric chemical vapor deposition (c-APCVD) used to synthesize a TiO_2 film with varying amounts of tungsten dopant and (b) the resulting film and the relative position of the Ti and W precursors introduced into the reactor during the deposition. Reprinted and adapted with permission from ref 139. Copyright 2011 American Chemical Society.

Tungsten(VI) chloride and titanium(IV) chloride were transported into separate baffles with separate ethyl acetate flow and, prior to entering the reactor, these gases were mixed to create a range of W/Ti ratio in the precursor. The resulting film with respect to the position of the precursor gases entering the reactor is shown in Figure 11b. Another method similar to c-APCVD that has been employed as a combinatorial method to prepare Sn doped- TiO_2 thin films is aerosol assisted chemical vapor deposition (AACVD).¹⁴⁰ Following synthesis, the photocatalytic activity was analyzed using an intelligent ink technique that will be discussed in section 5.

The application of high-throughput metal organic decomposition (MOD) that employs automated systems to prepare porous thin films of binary oxides was reported by Arai et al.¹²⁶ In this technique, metal ions were dispersed at the atomic level and stabilized by an organic compound, thereby minimizing precipitation. To facilitate the high-throughput process, a robotic arm was also employed to assist rapid transfer of the materials library from the synthesis apparatus into the furnace. A schematic of this system is shown in Figure 12. Two libraries

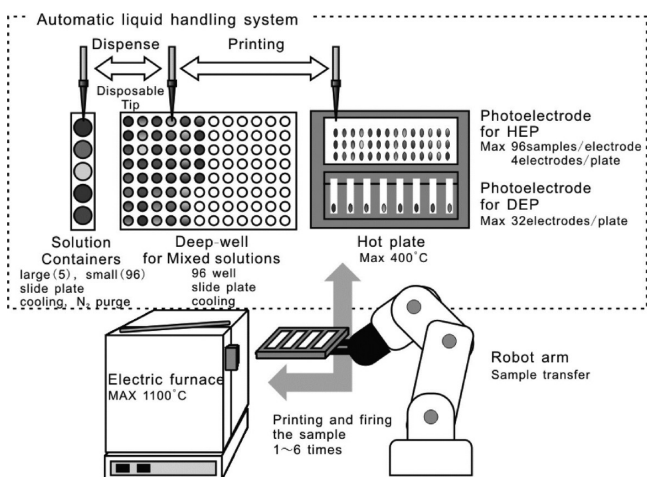


Figure 12. Schematic illustration of an automated liquid handling and printing system using a metal organic decomposition method, which includes the high-speed evaluation procedure (HEP) and detailed evaluation procedure (DEP). Reprinted with permission from ref 126. Copyright 2007 American Chemical Society.

for two different screenings were prepared. One library consisted of 42 samples per substrate (with a maximum of four substrates processed per experiment) for a high speed evaluation procedure (HEP), whereas the other library only comprised of 1 sample per substrate and was manually prepared for a detailed evaluation procedure (DEP). Precursor solutions in containers were first dispensed into the deep wells and then mixed. Both solution containers and deep wells were subsequently cooled, capped, and purged with dry N_2 . Then, a small amount of sample solution was printed on a conductive substrate and the photocurrent was subsequently measured. Although the primary focus of the work was on iron-based binary oxides, this setup was successfully applied to the printing of TiO_2 films, as a control experiment, using similar conditions.

Another combinatorial-feasible technique for material synthesis is electrochemical deposition. This method offers some advantages, particularly for high-throughput preparation because the synthesis variables can be directly controlled from variation in voltage, current density, and electrolyte.^{31,141} In the area of catalysis, McFarland's group has published several studies on the application of an automated electrochemical-based synthesis for depositing libraries of metal-oxide semiconductor thin films such as porous alumina membranes,¹⁴² WO_3 ,^{143,144} and mesoporous ZnO .¹⁴⁵ For TiO_2 films, they applied this technique to synthesize a 8×4 well array materials library comprising TiO_2 films with Au nanoparticles deposited on its surface using an automated pulsed electrodeposition technique.¹⁴¹ TiO_2 anatase films, as the cathodic substrate, were obtained by thermal oxidation at $400\text{ }^\circ\text{C}$ and $HAuCl_4 \cdot 3H_2O$ was employed as the Au precursor. The size of the Au nanoparticles was modulated by varying the deposition times as controlled by the number of pulses. Figure 13 shows schematics of the setups in two configurations: serial and parallel. In the serial electrochemical deposition system (Figure 13a), the synthesis is performed sequentially using an x , y , and z robotic stage, in which the electrodes (Pt and Ag wire serving as the counter and reference electrode, respectively) were dipped in each well one at a time. Meanwhile, an array of stainless steel counter electrodes was used in the parallel configuration (see Figure 13b). The parallel system allows

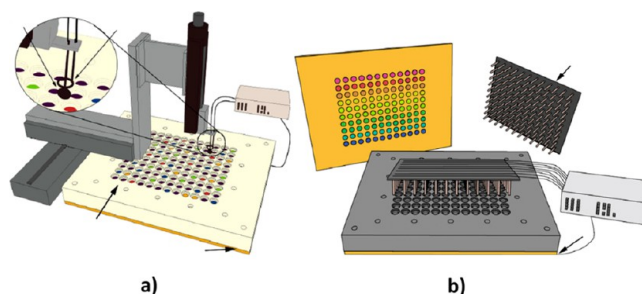


Figure 13. (a) Serial and (b) parallel configurations of an automated pulsed electrodeposition system for combinatorial synthesis. Reprinted and adopted with permission from ref 141. Copyright 2005 IOP Publishing.

faster deposition, although better control can be achieved using the serial configuration. For material diversity, deposition conditions, such as time, voltage, current, surfactant additives, and electrolyte, were varied accordingly.¹⁴¹ Such variation was easily achieved in the serial configuration, whereas only variation in voltage was possible in the parallel system. By employing a similar automated photoelectrochemical system, McFarland's group also developed a high-throughput screening setup which will be discussed later.¹⁴¹

Another interesting combinatorial method, as reported by Parkinson et al., involved the use of inkjet printing to deposit thin films of Fe-, Cu-, Cs-, Nd-, Co-, and Al-based oxide photoelectrodes on conducting glass for water splitting applications.¹²⁷ They printed overlapping patterns of metal oxide precursors from soluble metal salts onto a $SnO_2:F$ substrate using inkjet printer cartridges. The printing was repeated up to three times to obtain an adequate thickness. The resulting layer was then sintered at $500\text{ }^\circ\text{C}$ for 1 day to obtain the metal oxide film. The efficiency of the photoelectrodes for water splitting processes was assessed by measuring the photocurrent following irradiation of the samples with a laser. This method benefits from fast operation and low cost as no sophisticated robotic system is required. A deposition method using inkjet printing was also demonstrated by Liu et al. to create a library of mesoporous binary, ternary, and quaternary oxides for catalysis.¹⁴⁶

5. HIGH-THROUGHPUT PROPERTY SCREENING

The screening process of a number of materials within a certain library is a critical step, as it is required to produce high-yield results, as well as accuracy equivalent to that offered by conventional single sample testing methods. As previously mentioned, the first application of a combinatorial approach on solid-state materials library design was reported by Xiang et al. as inspired by the creation of an organic molecules library in biology.²⁴ Their results have successfully established a superconducting oxides library containing 128 materials prepared by thin film deposition and masking techniques. However, little focus was made on the screening process as opposed to the thin films material synthesis using the RF sputtering technique. Several studies on the application of high-throughput approaches for materials screening were reported in the following years. Many screening methods were mostly applied in search of reliable catalyst materials, especially in the form of solid state, consequently triggering the discovery of photocatalysts for environmental remediation.

Table 1. Overview of High-Throughput (HT) Photocatalytic Analytical Tools for Assessing the Photocatalytic Activity of TiO₂-Based Photocatalysts in Various Photocatalytic Reactions

HT-photocatalytic screening method	photocatalytic activity measurement tool	target compound	number of samples/ batch	number of samples/ batch	highlights of the findings	ref
parallel photodegradation of organic compound	HPLC	4-chlorophenol	45	45	doping with Tb, Mn, and Pr showed photocatalytic improvements	110
parallel photodegradation of organic compound	UV-vis spectroscopy	phenol	20	20	1.5 wt % Co loaded in TiO ₂ resulted in the highest degradation	109
discoloration	UV-vis spectroscopy	methylene blue	10	10	the coupling of rare earth oxides and P25 gives higher photocatalytic activity compared to pristine TiO ₂ when calcined at 800 °C because of the retardation of anatase to rutile transformation	147
fluorescence-based measurement	fluorescence camera	1,6-hexamethylenediamine	144	144	TiO ₂ doped with both Nb ₂ O ₅ and WO ₃ gave a stronger catalytic performance	106
CO ₂ detection	CO ₂ (infrared) detector	1,2 ethanediol, 1-dodecanol, 9-octadecenoic acid, and n-heptadecane	1	1	the degradation behavior of different organic compounds using P25 is dependent on the carbon composition and the light source used	148
hydrogen detection	gas chromatography	n.a. (catalyst powder was suspended on methanol/detonized water)	100	100	ternary metal oxide composition Al ₄₀ Bi ₄₀ Pb ₂₀ O _x was identified as the new lead photocatalyst	
discoloration	UV-vis spectroscopy	methylene blue	9	9	5.0 mol % of Ag-TiO ₂ produced the highest reaction rate	115
pH measurement	pH sensor	n.a.	9	9	thin films	
discoloration	UV-vis spectroscopy and photo scanner (followed by analysis using RGB Extractor)	intelligent ink	n.a.	n.a.	cobalt concentrations between 8.8 and 9 atom % attained the highest photocatalytic activities	123
electrochemistry cell	potentiostat	n.a.	32	32	trends in both red and green components in RGB color was shown to be related to the kinetics of photocatalytic reaction	138
photoelectrode	photocurrent measurement	n.a.	16	16	catalytic activity of Au-TiO ₂ for CO oxidation is affected by the particle size of Au	141
					the highest photocurrent was obtained at a TiO ₂ /WO ₃ mole ratio of 2:8	149

The scope of photocatalysis screening is mainly classified into two purposes: measurement of photocatalytic activity and evaluation of the photocatalyst material properties. Section 5.1 details the various photocatalytic test setups employed for photoactivity measurements, which are categorized according to the type of photocatalyst materials, that is, powder or thin films. The discussion includes the photoreactor design as well as the method applied to quantify the photodegradation of the target pollutant. Section 5.2 highlights the application of high-throughput analytical tools used for physical characterizations of the photocatalysts. More details will be given for the former since more studies have been reported in this area.

5.1. Photocatalytic Activity Measurement. Scientists have used several different techniques to determine the photocatalytic activity of their materials. Likewise, in high-throughput photocatalysis research, several analytical tools have been applied. Table 1 lists high-throughput photocatalytic measurement techniques that have been employed for characterizing the photocatalytic activity of TiO₂-based photocatalysts as published in various reports. The techniques and setups are detailed afterward.

5.1.1. Screening of Photocatalyst Powders. Maier's group was the first to report on the implementation of semiautomatic combinatorial systems, including both synthesis and screening, to evaluate a new library of photocatalyst powders.¹¹⁰ They utilized high performance liquid chromatography (HPLC) as the main characterization tool to assess the photocatalytic activity. Three sets of mixed-oxide material libraries, based on TiO₂, SnO₂, and WO₃, each consisting of 45 samples were prepared. For the photodegradation testing, 4-chlorophenol (4-CP) was chosen as the model pollutant. All samples within each library were diluted with 1 mL of 4-CP and subjected to visible light irradiation for 2.5 h, under agitation using a shaker (see Figure 14). The samples were subsequently centrifuged and the

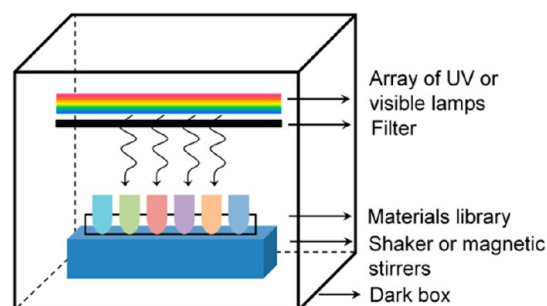


Figure 14. Schematic of a typical setup of a photocatalytic reactor for the irradiation of powder-based libraries using organic compounds or dyes as the model pollutant.

concentration of 4-CP was analyzed using an HPLC sampling robot. The results revealed that the addition of Tb, Mn, and Pr dopants to the TiO₂-based mixed-oxides library improved the photocatalytic activity. As for the SnO₂ library, a larger variety of dopant materials was found to increase the photodegradation conversion compared with that of the TiO₂ library. In contrast, only a few materials in the WO₃ library, improved the photocatalytic activity. Although being a facile method to apply, the procedure generated materials displaying phase irregularity: for instance, some materials were in powder form and others remained in a gel state. This influenced the photocatalytic measurements that were carried out directly after the final stage of the synthesis, that is, calcination. Although the

results indicated that the varied particle sizes obtained from the synthesis influenced the photocatalytic activity of the samples, no further characterization of the materials was provided to clarify the effect of such variations on the material properties. A similar photocatalytic reactor setup was also adapted and reported by several authors using different target pollutants; Sohn et al. reported the photocatalytic activity of TiO₂ photocatalysts doped with Pt, Cu, Fe, Co, and Ni using combinatorial techniques.¹⁰⁹ However, they employed UV-vis spectrometry to monitor the degree of photodegradation based on the change in the concentration of phenol following irradiation. The highest activity was achieved by Co-TiO₂ with a metal loading of 1.5 wt %.

Similar testing based on dye discoloration was performed by other groups.^{115,120,147,150} Gao et al. used methylene blue (MB) as a probe pollutant to investigate novel photocatalysts based on ABO₃ binary oxides (A = Y, La, Nd, Sm, Eu, Gd, Dy, Yb; B = Al, In) that are active under visible light.¹²⁰ After exposure, cubic YInO₃ and perovskite YAlO₃ were successfully identified as novel photocatalysts that showed potential application particularly for water splitting and toluene oxidation. Schmidt and co-workers used several other organic dyes (rhodamine B, malachite green, and acid blue) to assess the photocatalytic suitability of TiO₂ nanopowders doped with transition and rare metals.¹⁵⁰ Measurement of UV-vis absorbance is the most common technique used in dye discoloration-based methods for assessing their degradation. The application of UV-vis spectroscopy preceded by centrifugation of the samples generally offers the advantage of analyzing the change in the pollutant concentration. However, laborious work and prolonged processing time remain the downside of such treatments. This may become another bottleneck in high-throughput screening that should be taken into further consideration. Some authors reported the application of such a method for photocatalytic tests; however, only up to ten parallel reactors can operate at the same time.^{115,147} In addition, the use of dye photobleaching tests to determine the photocatalytic activity, particularly under solar or visible light irradiation, is often considered inappropriate because of the dye-photosensitization. In this process, electron injection from the electronically excited state of the dye, D*, into the conduction band of the photocatalyst produces an oxidized dye radical, D^{•+}, which is unstable and able to decompose into bleached products.^{151–153} Furthermore, Mills et al. also reported that the photobleaching of dye (e.g., methylene blue) is not equivalent to the rate of mineralization, as the latter occurs over a longer time scale.¹⁵⁴

Detection of the photocatalytic reaction products, such as CO₂, can also be applied to characterize the degree of photocatalytic activity in a rapid fashion. Such an approach has been reported by Ritter et al.¹⁴⁸ By fabricating a custom-built apparatus, they were able to quantify the degradation behavior of four different nonvolatile organic compounds (1,2-ethanediol, 1-dodecanol, 9-octadecenoic acid, and *n*-heptadecane) under various illumination conditions using Aeroxide P25 nanoparticles as the photocatalyst. The yield of CO₂ evolution is defined as the ratio of the mass of the CO₂ produced (measured using a CO₂ detector) to the equivalent amount of CO₂ generated in a complete mineralization. This technique has also been successfully applied to investigate the photocatalytic degradation of formaldehyde on the irradiated surfaces of fibers and fabrics containing TiO₂ photocatalyst.¹⁵⁵ This novel method offers a relatively quick and straightforward

screening method (45 min purging, 15 min irradiation, and 60 min purging). However, the ability for simultaneous characterization of multiple samples remains the significant challenge for high-throughput characterization to date. A similar high-throughput characterization technique using photocatalyst powders based on the detection of reaction product was demonstrated by Maier's group.¹¹¹ A mixed metal oxide library prepared from 29 different liquid precursors was generated and analyzed by gas chromatography techniques to discover new catalyst materials for hydrogen production from aqueous methanol solution. In their high-throughput setup, 100 gas chromatography vials (which were also used as reaction vessels, containing the photocatalyst) were irradiated with a 500 W (covering UVA and visible range) light bulb. These vials were placed 20 cm away above the light source and fans were used to maintain the temperature. The setup is depicted in Figure 15.

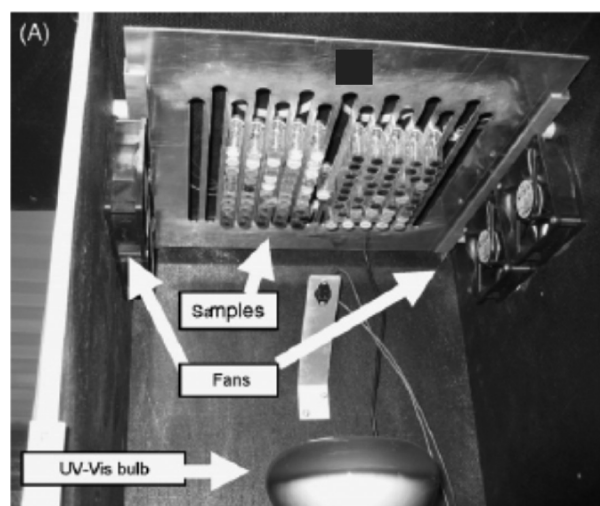


Figure 15. High-throughput setup that enables simultaneous irradiation of multiple samples. Reprinted with permission from ref 111. Copyright 2007 Elsevier.

After irradiation, the hydrogen content within each vial was measured. The screening results indicated that $\text{Al}_{40}\text{Bi}_{40}\text{Pb}_{20}\text{O}_x$ was the most active composition, with a relatively broad light absorption in the visible light spectrum, compared to the prepared carbon doped TiO_2 that was included as a reference catalyst.

The effectiveness of running different parallel photocatalytic reactor setups for TiO_2 nanopowders was recently examined by Thompson et al.¹¹⁵ Three parallel screening methods, with each reactor containing the same metal-doped TiO_2 nanoparticles, were studied. The dopants being analyzed are Zn^{2+} , Sr^{2+} , La^{3+} , Ag^+ , and Pr^{3+} . The three screening methods involved: methylene-blue (MB) degradation as characterized by UV-vis-spectroscopy; propan-2-ol oxidation as measured by gas-liquid chromatography; and degradation of dichloroacetic acid (DCA) in aqueous solution as measured by the concentration of chloride ions. In addition to discovering the best combination of photocatalysts, the feasibility of these reactor setups as high-throughput photocatalytic screening methods was assessed. Comparative studies of the different reactors revealed that the effect of doping, including dopant type and concentration, was determined by the reaction being monitored. For example, the best result from the MB degradation method was attained by 5.0 mol % of Ag-doped

TiO_2 , whereas 0.5 mol % of La doping was shown to be superior for propan-2-ol oxidation and DCA degradation. On the other hand, all three methods consistently showed the detrimental effect of Pr doping on the photocatalytic activity of TiO_2 . In terms of high-throughput feasibility, it was concluded that only MB and DCA photodegradation methods were suitable for parallel screening, as the propan-2-ol method required gas-liquid chromatography conducted separately for every data point collected for each sample. However, some challenges in the MB and DCA photodegradation methods remain. For the measurement of MB discoloration, every sample needs to be centrifuged to remove the particulates prior to the UV-vis measurement. As previously mentioned, such treatment would increase the processing time and would be impractical for a large number of samples. While the DCA method offers more feasibility for large sample numbers, as the reaction progress can be monitored continuously via a data logger, the results are likely to be sensitive to the surface area of the photocatalyst.

The application of fluorescence imaging to analyze the photodegradation of aromatic polymer libraries, combined with rutile TiO_2 and carbon black as pigments, in 11 levels of weatherability tests was reported by Potyrailo et al. in 2002.¹⁵⁶ The same concept was also employed by Zhou and co-workers who used a fluorescent compound as the probe indicator for assessing photocatalytic activities under visible light.^{106–108} 1,6-Hexamethylenediamine ($\text{NH}_2(\text{CH}_2)_6\text{NH}_2$) was used as it is able to produce fluorescent products when it reacts with fluorescamine upon UV light illumination. Thus, the change in fluorescence produced, as a result of 1,6-hexamethylenediamine decomposition, was used as an indicator for measuring photocatalytic activity. The characterization techniques involved two different reactors. Reactor 1, the photocatalytic reaction chamber, was an enclosed box containing a polytetrafluoroethylene (PTFE) reaction plate and six mercury lamps producing visible light (Figure 16a). Reactor 2 was used

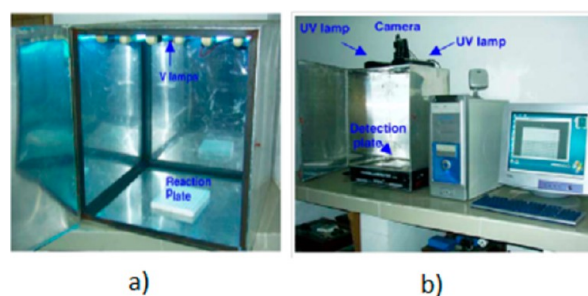


Figure 16. Fluorescence-based imaging setup for photodegradation measurements that consists of (a) photocatalytic reactor (reactor 1) and (b) fluorescence detection setup (reactor 2). Reprinted with permission from ref 106. Copyright 2006 Elsevier.

as the detection chamber, which features a detection plate, UV lamps, and CCD camera (Figure 16b). The measurement method is briefly explained. First, the catalyst materials and aqueous solution of 1,6-hexamethylenediamine were placed in the wells of the PTFE reaction plate in Reactor 1 and these mixtures were kept in the dark for 20–30 min to equilibrate. Then, 30 μL of each solution was transferred to the detection plate in reactor 2, and 30 μL of fluorescamine/DMF solution was subsequently added and then set aside for 10 min at room temperature. A picture of the detection plate was subsequently

taken and used as the initial data (referred to as data B). Meanwhile, the rest of the catalyst and 1,6-hexamethylenediamine mixtures in reactor 1 were illuminated with visible light to initiate the photocatalytic process. Pictures (in reactor 2) were taken at given irradiation times (referred to as data C) to monitor the photocatalytic process. The change in 1,6-hexamethylenediamine concentration in this method was calculated as $(\text{data B} - \text{data C})/(\text{data B} - \text{data A})$, where data A is the data obtained from the image of the blank detection plate. Several libraries containing a large number of materials from a combination of TiO_2 , ZrO_2 , Nb_2O_5 , WO_3 , V_2O_5 , and MoO_3 were prepared and investigated.^{106–108} The authors concluded that TiO_2 -doped with both Nb_2O_5 and WO_3 gave the best catalytic performance. In these studies, Zhou et al. demonstrated the potential of the fluorescence imaging method for discovering new catalytic materials.

In general, UV–vis spectroscopy and chromatography (either liquid or gas) are the most common analytical tools employed for high-throughput screening of photocatalyst powders. Although these tools do not allow concurrent measurements to be made, the sequential measurements of several samples can be achieved in a relatively short time. Therefore, this set up is naturally feasible for high-throughput experimentation, although it may be relatively slow when libraries with a significant number of samples are involved. An alternative reading method such as a plate reader, which is widely used in pharmaceutical and biotechnological industrial research studies, could be a promising solution for this issue. This apparatus is able to simultaneously measure the absorption (or other features such as fluorescence and luminescence) of multiple samples in small scale, which are placed in arrays of wells within a microtiter plate. This technique has been applied by Mallouk et al. to demonstrate rapid screening of photolysis reactions using $\text{IrO}_2 \cdot x\text{H}_2\text{O}$ colloidal catalysts.¹⁵⁷

5.1.2. Screening of Photocatalyst Thin Films. A unique photocatalytic screening technique based on pH variation was published in 2002 by Nakayama and co-workers.¹²³ The aim was to characterize the photocatalytic activity of 3×3 TiO_2 libraries doped with cobalt at various concentrations. The library was fabricated using combinatorial laser molecular beam epitaxy (MBE) as discussed in section 4.2. TiO_2 -doped with cobalt concentrations between 8.8 and 9 atom % displayed high photocatalytic activities under visible light. Rather than monitoring the degradation of reactant pollutants, the main concept was to observe the amount of proton species produced during the photocatalytic reactions. By placing a ferric sulfate liquid film on the surface of the doped- TiO_2 library, the reductive path of H^+ can be inhibited, as reduction of Fe^{3+} to Fe^{2+} will take place instead. Hence, the quantity of the originally produced H^+ is proportional to the photocatalytic activity. The characterization was conducted as follows: first, ferric sulfate solution was placed on each sample and then irradiation was performed. The library plate was subsequently dried, inverted, and placed upside down on top of electrolyte gel (to isolate the protons) above a pH image sensor. The proton quantity was calculated from the pH, as measured by photocurrent, on the device as shown schematically in Figure 17. Additionally, the photocatalytic activities could be visually assessed according to the image colors. However, this method has certain limitations. First, the pH imaging only supports two-dimensional measurements, which limit the possibility of establishing larger materials libraries with combinations of

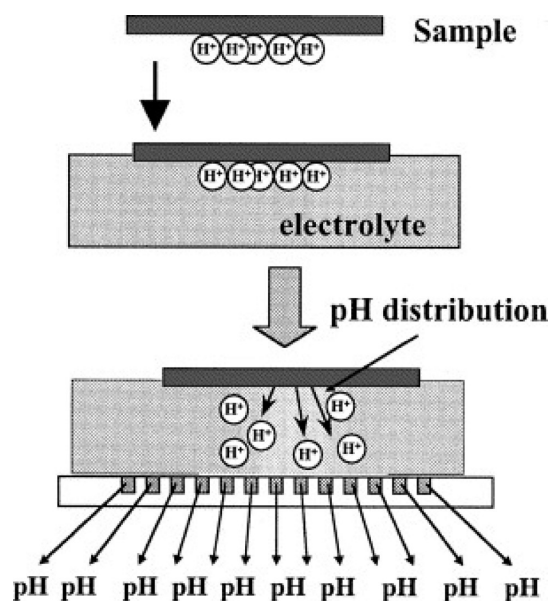


Figure 17. Mechanism of proton diffusion from the sample into the pH sensor, following the addition of ferric ions in order to replace the reduction path of H^+ , thereby allowing the subsequent measurement of the generated protons, isolated with the aid of the electrolyte gel layer. Reprinted with permission from ref 123. Copyright 2002 Elsevier.

more than one dopant material (examples of three-dimensional characterization is given in these studies^{106–108,110}). Also, this technique is not feasible for hydrogen production, as such process requires reduction energy that is higher than the potential energy of the ferric ion reduction.

Parkin and co-workers also assessed the photocatalytic activity of self-cleaning glass based on color change, that is, by monitoring the conversion of resazurin (blue) to resorufin (pink) under UV irradiation using an intelligent ink deposited from a felt-tipped pen.¹³⁸ This ink was an aqueous solution of hydroxyl ethyl cellulose (HEC) polymer, glycerol, and resazurin redox dye. When the semiconductor is coated with the intelligent ink and illuminated, the sacrificial electron donor acts as a hole trap and subsequently reduces the resazurin-blue dye to its pink colored form, that is, resorufin. Such color transformation occurs rapidly (see Figure 18). The color change was subsequently monitored by a digital photographic method under illumination and the resulting image was

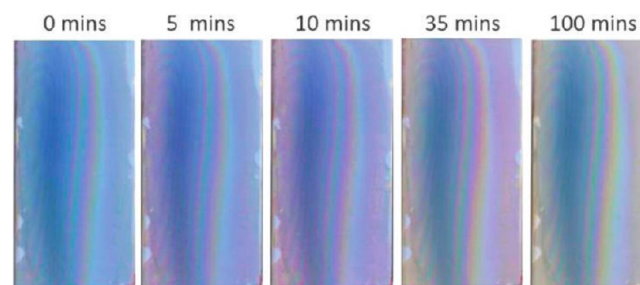


Figure 18. Color changes observed on a nitrogen-doped TiO_2 film with gradating nitrogen composition upon the application of intelligent ink grids on the film surface over several periods of time. The color transformation indicates the photocatalytic degradation within the underlying film. Reprinted with permission from ref 139. Copyright 2011 American Chemical Society.

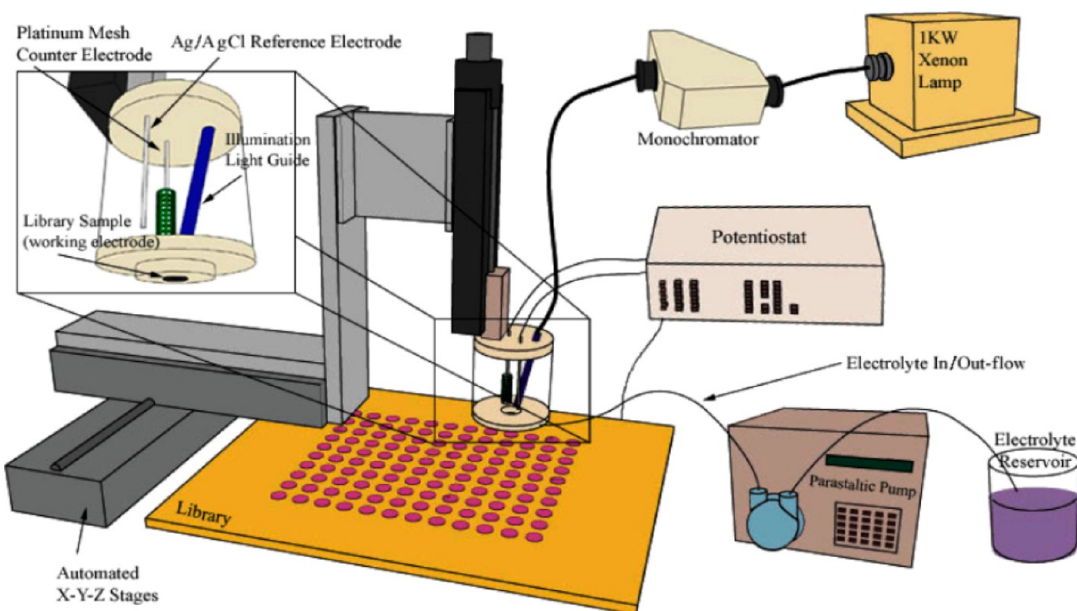


Figure 19. High-throughput screening setup using an automated photoelectrochemical system. A cell containing the electrodes and light source (magnified image) is moved across the library to measure the photocurrent of each sample. Reprinted with permission from ref 141. Copyright 2005 IOP Publishing.

extracted into red-green-blue data using custom-made software (RGB Extractor) to enable the mapping of photocatalytic activity throughout the film. The advantage of this method lies in the visual observation that can be easily performed using an imaging method and thus eliminates the necessity of a robotic-based apparatus. This has been applied to different substrates, that is, titania thin film composites doped with nitrogen,^{124,138} tungsten,¹³⁹ and tin oxide.¹⁴⁰ The resazurin dye was typically sprayed on top of the thin-film followed by irradiation and monitoring of the digital images.^{139,140} In some cases, a felt tip pen filled with intelligent ink was also used to draw grids on TiO_2 thin film to monitor each region individually.^{138,158}

As mentioned in section 4, McFarland and co-workers have developed an automated photoelectrochemical screening system for evaluating the photocurrent properties of materials within a library using electrochemical probes.^{141,143–145} The setup employed for assessing the photoactivity of Au/TiO_2 materials and other metal-oxide semiconductor catalysts is illustrated in Figure 19. A computer controlled probe containing Pt counter and Ag/AgCl reference electrodes was employed to measure the photoelectrochemical properties in each cell in which sodium acetate was used as the electrolyte. The illumination was performed using a 1 kW Xe lamp through an optical cable. The degree of photoactivity was measured as the difference between the current (measured under illumination) and the dark current (in the absence of light). The photodegradation rate was closely related to the particle size of the highly dispersed Au, with small Au nanoparticles (diameter <10 nm) showing relatively higher photoactivities.

Similar to photoelectrochemical-based approaches, Woodhouse et al.¹²⁷ and Arai et al.¹²⁶ evaluated the photoactivity of iron-based materials for photoelectrolysis via photocurrent measurements. The electrodes containing thin films were immersed in the electrolyte. Every sample was subsequently scanned with focused light while a constant potential was applied and the photocurrent was measured simultaneously. Likewise, a similar approach was recently reported by Xie et al.

to assess the photoactivity of TiO_2 composites, that is, $\text{TiO}_2/\text{WO}_3/\text{MnO}_2$ ¹⁴⁹ and $\text{TiO}_2/\text{ZnO}/\text{Fe}_2\text{O}_3$.¹⁵⁹ Rather than using a model pollutant to demonstrate the photodegradation, the recombination rate within the semiconductor was analyzed and used as a measure of the photoactivity. This was performed by detecting the population of photoexcited electron-hole pairs that survived recombination through the photocurrent measurement. The measured photocurrent is determined by the number of electrons that reach the electrode. A library of materials containing 66 composite samples made from three different oxides was prepared with specific mole ratio patterns, the so-called “ingredient triangle” (see Figure 20). The combination of oxide semiconductor powders were mixed using an agate ball milling tank at certain ratios and then combined with an organic solvent as a thickening and rheological agent to obtain paste. The paste was then printed onto a gold interdigital electrode preprinted on an alumina substrate using a screen printing method. Figure 21 shows a

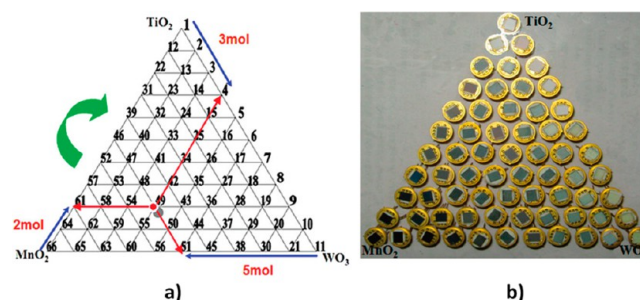


Figure 20. (a) “Ingredient triangle” materials library which consists of 66 materials composed of different mole ratios. For example, point 49 represents a mole ratio of 2:3:5 for $\text{TiO}_2/\text{WO}_3/\text{MnO}_2$ (as shown by the red dot and arrows). (b) The materials library was prepared as thin films, where each sample was separately deposited on a Au-preprinted alumina substrate as the conducting electrode (right). Reprinted and adapted with permission from ref 149. Copyright 2010 American Chemical Society.

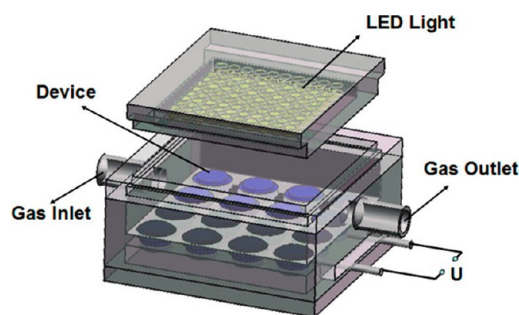


Figure 21. Schematic diagram of the high-throughput apparatus used for measuring photoelectric current of multiple semiconductor samples. Reprinted with permission from ref 149. Copyright 2010 American Chemical Society.

schematic illustration for the screening setup. The quick, simultaneous and separate photocurrent measurement of over 16 samples can be achieved with this setup. The testing procedures are as follows: first, the conductivity of the semiconductor is obtained by measuring the dark current under an applied bias voltage for a few seconds. Then, the sample is illuminated at a certain wavelength to generate photoexcited electron–hole pairs while the applied bias voltage helps to improve the charge separation. Four different light sources in the form of light emitting diodes were employed to analyze the photoresponse. Finally, the light source is turned off rendering a quick charge recombination, which causes the photocurrent to decrease rapidly. The maximum photocurrent measured at the cutoff point (i.e., when the light is turned off immediately before the photocurrent starts to decrease) is chosen as the main parameter to compare the photoelectric response among the samples within the library. As expected, each sample behaves differently upon irradiation with different light sources and the optimum composition of the materials can be obtained for each light condition. This technique provides an interesting insight into photocatalysis research, particularly in regards to the charge transport. However, direct photo-degradation evidence of a pollutant would be beneficial to support the findings from this method since this technique lacks an actual photocatalytic reaction.

5.2. Materials Characterization. This section reviews the current literature on the use of high-throughput screening techniques for characterizing the properties of materials, and is not limited to TiO₂. As part of their technological development, some material characterization techniques have been naturally upgraded to allow multiple functional materials to be elucidated simultaneously. Characterization of the material is very powerful as either a primary or secondary screening step, since it provides further insight into the material properties, which are strongly linked with the photocatalytic activity.

For the case of lab-based X-ray diffraction (XRD) and X-ray fluorescence (XRF) techniques, two main problems arise in analyzing combinatorial libraries, that is, the limited brightness of the X-ray source, which can affect the sensitivity and accuracy, and second, the relatively long processing time, hence lowering the overall throughput.¹⁶⁰ To overcome these obstacles, various modifications can be applied, such as using parallel beams, a convergent beam, divergent beam, or synchrotron microbeam.³⁸ In 1998, Isaacs et al. proposed the application of a synchrotron X-ray microbeam to characterize the chemical composition (using XRF), crystallographic structure (using XRD), and valence states (using near edge

X-ray absorption fine structure spectroscopy, NEXAFS) of rare earth thin film compounds.¹⁶¹ They also introduced the use of elliptically bent mirrors that produced an improved spot size with increased flux, which allows a larger area for phase identification. Later, Ohtani et al. designed an X-ray diffractometer that can spatially measure the XRD spectra of epitaxial thin films integrated on a substrate.¹⁶² Meanwhile, Luo et al. demonstrated an integrated measurement setup featuring the application of energy dispersive XRD (EDXRD), XRF, and X-ray photoluminescence by employing a polycapillary based X-ray.¹⁶⁰ Subsequent improvements in this analytical area have continued to be reported, enabling further characterization of both thin films and powders.^{163–165} In the area of TiO₂ photocatalyst research, Woo et al. demonstrated the use of combinatorial microbeam XRD featuring a parallel micro-diffractometer with XYZ stage and Gobel mirrors to analyze the crystal structure of 20 doped-TiO₂ samples placed on top of a Si wafer.¹⁰⁹ They reported that all 20 samples were analyzed within 3 h.

Another common technique used for characterizing catalyst materials is infrared (IR) thermography. Moates et al. reported the use of in situ IR thermography screening to select potential metal catalysts impregnated on γ -alumina pellets, based on the heat released from the hydrogen oxidation catalytic activities during the process.¹⁶⁶ Though their noninvasive IR thermographic method was able to identify active catalysts based on the emissivity level, the heat and mass transport effect showed a significant influence on the pellet temperature, which further limits the data interpretation. One factor causing this was the increase in the temperature of the reactants and products, which was reflected on the library surface and obstructed the IR emission image. Also, as the temperature difference between the catalyst and library surfaces decreased with the catalyst mass, it was difficult to measure the heat dissipation rate of the small pellets. The sensitivity at lower temperatures had also been an issue. The emissivity and reflectance differences in the catalysts and library surfaces may lead to misinterpretations, as the photon intensity captured by the camera may vary although the surface temperature is the same. To overcome these limitations, Maier and his group came up with some improvements. A preliminary image correction was carried out before the catalytic reaction was started and a low reflectance slate plate was used as the library substrate. The correction accounted for the heat emitted within the chamber before the feed gas was released and the heat produced from the reaction is liberated.¹⁶⁷ Thus, quantification of the temperature difference specific to the catalytic activity of the heterogeneous catalysts was possible. A larger reactor featuring 200 wells and a pipetting robot was also built in the following studies to further improve the system.¹⁶⁸ IR thermography has remained a popular method to discover novel catalyst materials. Loskyll et al. recently provided a review on high-throughput IR thermography and its development.¹⁶⁹ Significant improvements have also been reported to allow parallel screening in Fourier Transform Infrared (FTIR) spectroscopy. In their design, Snively et al. demonstrated the application of rapid-scan FTIR spectral imaging to perform parallel studies of the adsorbate and gas-phase reaction products of catalyst libraries.^{170,171}

Mass spectrometry is one of the most popular tools to have been optimized for high-throughput experimentation, especially in catalyst research. Various modifications such as using microprobes and online mass spectrometry,¹⁷² multi stream

mass-spectrometry screening (MSMSS) for parallel testing of secondary heterogeneous catalyst libraries,¹⁷³ and time-of-flight (TOF) mass spectrometry coupled with gas chromatography (GC),¹⁷⁴ have been reported. Mass spectrometry combined with chromatography is usually more common, including in the area of combinatorial chemistry, as it is a powerful tool for identifying substances on the molecular level based on molecular structure.

Nuclear magnetic resonance (NMR) has also been reported to support combinatorial research.¹⁷⁵ As another alternative for rapid screening, Senkan introduced a screening technique based on the photoionization of product molecules, in the form of benzene, within solid-state catalyst sites upon the application of tunable ultraviolet laser beam, so-called resonance-enhanced multiphoton ionization (REMPI).³⁰ In this technique, photons are detected by an array of microelectrodes located in close proximity above the sample libraries. When an UV laser beam is passed above the sample, these microelectrodes collect the signal. The photon frequency of the applied beam corresponds to the selectivity of the reaction products. This technique offers a rapid selectivity; however, the challenge is to determine the laser frequency used to stimulate the photoionization process of the product molecule (especially other than benzene) if it is to be applied for a different range of materials. Thus, the spectral properties of the material of interest need careful consideration.

6. CONCLUSION

Research studies examining the development of an efficient photocatalyst can be overwhelming since photocatalytic activity is influenced by a large array of diverse factors. Therefore, combinatorial techniques offer an effective route for either discovering novel or optimizing any existing photocatalyst materials. Various high-throughput techniques have been developed to improve the pace of research in the photocatalysis area, including studies of titania-based photocatalysts. While TiO₂ has been widely established as a benchmark photocatalyst, optimization of this material through modification has demonstrated promising results and has the potential to create many new possibilities. By employing combinatorial approaches, rapid improvement of TiO₂ photocatalysts has been made possible in a more efficient way. The reported studies discussed herein demonstrate how much progress has been made in the high-throughput study for the optimization of TiO₂ photocatalysts within the past few years.

In planning high-throughput research, considerations for selecting appropriate rapid synthesis and characterization methods are inseparable. This should be taken into account when determining the phase of the TiO₂ photocatalyst library, that is, in the form of dispersed powder or thin films, before performing the actual high-throughput experiments. Combinatorial synthesis of TiO₂ has been demonstrated using sol-gel and CHFS techniques. Sol-gel synthesis has been a popular method of choice for many groups for preparing TiO₂-based nanopowders. While some groups have applied robotic tools to upgrade the system, conventional sol-gel syntheses have been reported for preparing a large group of materials library. Parallel solution combustion synthesis and gas flame phase synthesis are also shown to be feasible alternatives for combinatorial TiO₂ synthesis. On the other hand, research in high-throughput TiO₂ thin films synthesis is more technologically developed as it involves more complex setup and more diverse techniques compared with the high-throughput synthesis of TiO₂ powders. The reported techniques include MBE, CVD, and electro-

chemical deposition. One of the reasons behind the advanced progress of thin films synthesis compared to powder synthesis is presumably affected by the rapid development of combinatorial synthesis for catalysis. Although powder photocatalysts are usually more advantageous for photocatalytic reactions owing to their higher surface area, more complicated treatments are generally associated with powders in contrast to thin films. For instance, the use of powders usually requires additional treatments such as separation from the suspension. However, variation in properties in the sol-gel synthesized powder libraries is normally easier to achieve using relatively simple modifications. Contrarily, combinatorial deposition of TiO₂ thin films mostly involves complex equipment for physical depositions that would require higher financial investment.

The number of publications in high-throughput TiO₂ (and other materials) photocatalytic screening to date has somewhat outnumbered the quantity of published reports on high-throughput synthesis. This implies that the demand for high-throughput screening at the application stage is still considered a more important issue. Some of the works reported the use of sophisticated and automated systems and others have also reported the application of basic self-developed equipment. Different methods have been reported and can be grouped into several approaches: i.e., pollutant degradation, change of color, fluorescence intensity, pH imaging, detection of reaction products, and photocurrent measurements. Some of the aforementioned techniques demonstrated a direct photocatalytic reaction (such as using target pollutant or dye discoloration techniques), while others provided alternative techniques that served as an indirect photocatalytic indicator (such as fluorescence, pH, and photocurrent measurements). Although the latter seems to be a quick screening method to assess the photocatalytic activity of the catalyst, an actual photocatalytic reaction upon interaction with the target pollutant would be beneficial to provide evidence of the reliability of the proposed technique. Another factor that needs to be taken into consideration in designing a high-throughput photocatalytic screening system is the practicality of the photoreactor design. One of the future challenges will be to design a testing system in such a way that the outcome rate of the reaction can be well-matched to that of the analysis. Often, the photocatalytic reactions were conducted simultaneously in a large batch, while the analysis was conducted as a sequential process. Thus, the overall screening process was slowed down and, consequently, precludes further adaptation into larger scale applications, for example at the industrial level. The application of an imaging-based screening method provides a good example to overcome this problem, although to date, it has been reported primarily for thin-film based photocatalysts.

In high-throughput photocatalyst research, knowledge and ability to perform rapid materials characterization is also beneficial. Thorough understanding of the materials properties and the ability to assess them in parallel, therefore, would be essential to reach the decision to create bulk quantities within a reasonable time. However, the application of high-throughput instruments for materials characterization in the photocatalysis area has drawn less attention (compared with the study of parallel photocatalytic screening) as this is commonly performed in a low-throughput manner.

To date, studies on the combinatorial synthesis and high-throughput screening of TiO₂ mostly focus on the optimization of TiO₂ through doping with other materials, mainly noble, transition, and rare earth metals. While the combinatorial

doping of TiO₂ with nonmetal anions and its high-throughput screening have been less frequently reported, this doping strategy holds much promise for the future as it can reduce the materials cost. Based on the reported high-throughput studies to date, it is difficult to make a direct comparison between the enhancement in the photocatalytic activity obtained from cation and anion doping, because the reports mostly focused on a certain group of dopants. Thus, it would be interesting to see such comparative work in the future. Also, in contrast, not many have been reported in the scope of morphological manipulation of TiO₂. As such, combining material properties and morphological modifications using a combinatorial approach would be a challenge for future research. The main task would therefore arise from adapting the conventional synthesis into the combinatorial process. In this regards, modification of the sol-gel synthesis would be a promising way to start.

In addition to the optimization of the synthesis and screening process, high-throughput experiments often require sophisticated computational tools, including suitable software, to control the experimental procedure as well as for advanced data mining, storage, and analysis. This is particularly useful when the data resulting from high-throughput experiments are complex and abundant due to the inclusion of numerous parameters or any substantial variations. Also, automation of the whole process often becomes a necessity to improve the overall control. A high degree of control is imperative during synthesis and screening to avoid any unnecessary variations that could introduce uncontrolled parameters across the library. Therefore, research in the high-throughput area, including the area of TiO₂ photocatalysis, may expand into multidisciplinary fields as it often requires a combination of knowledge from the areas of materials science, chemistry, physics, engineering, and informatics for data mining and processing. Advances in these areas will lead to new opportunities in the development of novel high-throughput systems for the study of TiO₂ and other photocatalysts in the future.

AUTHOR INFORMATION

Corresponding Author

*E-mail: rcaruso@unimelb.edu.au

Notes

The authors declare no competing financial interest.

ACKNOWLEDGMENTS

This work was financially supported by the CSIRO Office of the Chief Executive (OCE) Science Leader scheme. Dr. Maryline Chee Kimling and Dr. Nicholas M. K. Tse are thanked for giving feedback on the manuscript. N.M.N. acknowledges the support of Melbourne International Research and Melbourne Materials Institute-CSIRO PhD Materials Science top-up scholarships. R.A.C. is a recipient of Australian Research Council Future Fellowship (grant number FT0990583).

REFERENCES

- (1) Gratzel, M. Artificial photosynthesis: Water cleavage into hydrogen and oxygen by visible-light. *Acc. Chem. Res.* **1981**, *14*, 376–384.
- (2) Gratzel, M. Hydrogen-production by interaction between visible-light and water in micro-heterogeneous systems. *J. Chim. Phys. Phys.-Chim. Biol.* **1981**, *78*, 1–5.

- (3) Walter, M. G.; Warren, E. L.; McKone, J. R.; Boettcher, S. W.; Mi, Q.; Santori, E. A.; Lewis, N. S. Solar water splitting cells. *Chem. Rev.* **2010**, *110*, 6446–6473.

- (4) Armelao, L.; Barreca, D.; Bottaro, G.; Gasparotto, A.; Maccato, C.; Maragno, C.; Tondello, E.; Stangar, U. L.; Bergant, M.; Mahne, D. Photocatalytic and antibacterial activity of TiO₂ and Au/TiO₂ nanosystems. *Nanotechnology* **2007**, *18*, 375709.

- (5) Folli, A.; Pade, C.; Hansen, T. B.; De Marco, T.; Macphee, D. E. TiO₂ photocatalysis in cementitious systems: Insights into self-cleaning and depollution chemistry. *Cem. Concr. Res.* **2012**, *42*, 539–548.

- (6) Nair, M.; Luo, Z. H.; Heller, A. Rates of photocatalytic oxidation of crude-oil on salt-water on buoyant, cenosphere-attached titanium-dioxide. *Ind. Eng. Chem. Res.* **1993**, *32*, 2318–2323.

- (7) Yue, X. Q. Effect of ZnO-loading method on adsorption and decomposition capacities of expanded graphite/ZnO composites for crude oil. *Adv. Mater. Res.* **2011**, *284–286*, 173–176.

- (8) Kwon, S.; Fan, M.; Cooper, A. T.; Yang, H. Q. Photocatalytic applications of micro- and nano-TiO₂ in environmental engineering. *Crit. Rev. Environ. Sci. Technol.* **2008**, *38*, 197–226.

- (9) Cai, R.; Hashimoto, K.; Kubota, Y.; Fujishima, A. Increment of photocatalytic killing of cancer-cells using TiO₂ with the aid of superoxide-dismutase. *Chem. Lett.* **1992**, 427–430.

- (10) Tian, C.-Y.; Xu, J.-J.; Chen, H.-Y. A novel aptasensor for the detection of adenosine in cancer cells by electrochemiluminescence of nitrogen doped TiO₂ nanotubes. *Chem. Commun.* **2012**, *48*, 8234–8236.

- (11) Hoffmann, M. R.; Martin, S. T.; Choi, W. Y.; Bahnemann, D. W. Environmental applications of semiconductor photocatalysis. *Chem. Rev.* **1995**, *95*, 69–96.

- (12) Linesbigler, A. L.; Lu, G. Q.; Yates, J. T. Photocatalysis on TiO₂ surfaces: Principles, mechanisms, and selected results. *Chem. Rev.* **1995**, *95*, 735–758.

- (13) Su, C.; Tseng, C. M.; Chen, L. F.; You, B. H.; Hsu, B. C.; Chen, S. S. Sol-hydrothermal preparation and photocatalysis of titanium dioxide. *Thin Solid Films* **2006**, *498*, 259–265.

- (14) Wold, A. Photocatalytic properties of TiO₂. *Chem. Mater.* **1993**, *5*, 280–283.

- (15) Hashimoto, K.; Irie, H.; Fujishima, A. TiO₂ photocatalysis: A historical overview and future prospects. *Jpn. J. Appl. Phys.* **2005**, *44*, 8269–8285.

- (16) Simonsen, M. E.; Jensen, H.; Li, Z.; Søgaard, E. G. Surface properties and photocatalytic activity of nanocrystalline titania films. *J. Photochem. Photobiol., A* **2008**, *200*, 192–200.

- (17) Zhang, R.; Elzatahry, A. A.; Al-Deyab, S. S.; Zhao, D. Mesoporous titania: From synthesis to application. *Nano Today* **2012**, *7*, 344–366.

- (18) Potyrailo, R.; Rajan, K.; Stoewe, K.; Takeuchi, I.; Chisholm, B.; Lam, H. Combinatorial and high-throughput screening of materials libraries: Review of state of the art. *ACS Comb. Sci.* **2011**, *13*, 579–633.

- (19) Pollack, S. J.; Jacobs, J. W.; Schultz, P. G. Selective chemical catalysis by an antibody. *Science* **1986**, *234*, 1570–1573.

- (20) Lerner, R. A.; Benkovic, S. J.; Schultz, P. G. At the crossroads of chemistry and immunology: Catalytic antibodies. *Science* **1991**, *252*, 659–667.

- (21) Tramontano, A.; Janda, K. D.; Lerner, R. A. Catalytic antibodies. *Science* **1986**, *234*, 1566–1570.

- (22) Fodor, S. P. A.; Read, J. L.; Pirrung, M. C.; Stryer, L.; Lu, A. T.; Solas, D. Light-directed, spatially addressable parallel chemical synthesis. *Science* **1991**, *251*, 767–773.

- (23) Houghten, R. A.; Pinilla, C.; Blondelle, S. E.; Appel, J. R.; Dooley, C. T.; Cuervo, J. H. Generation and use of synthetic peptide combinatorial libraries for basic research and drug discovery. *Nature* **1991**, *354*, 84–86.

- (24) Xiang, X. D.; Sun, X. D.; Briceno, G.; Lou, Y. L.; Wang, K. A.; Chang, H. Y.; Wallacefreedman, W. G.; Chen, S. W.; Schultz, P. G. A combinatorial approach to materials discovery. *Science* **1995**, *268*, 1738–1740.

- (25) Danielson, E.; Golden, J. H.; McFarland, E. W.; Reaves, C. M.; Weinberg, W. H.; Wu, X. D. A combinatorial approach to the discovery and optimization of luminescent materials. *Nature* **1997**, *389*, 944–948.
- (26) Sun, X. D.; Wang, K. A.; Yoo, Y.; Wallace-Freedman, W. G.; Gao, C.; Xiang, X. D.; Schultz, P. G. Solution-phase synthesis of luminescent materials libraries. *Adv. Mater.* **1997**, *9*, 1046–1049.
- (27) Sun, X. D.; Gao, C.; Wang, J. S.; Xiang, X. D. Identification and optimization of advanced phosphors using combinatorial libraries. *Appl. Phys. Lett.* **1997**, *70*, 3353–3355.
- (28) Briceno, G.; Chang, H. Y.; Sun, X. D.; Schultz, P. G.; Xiang, X. D. A class of cobalt oxide magnetoresistance materials discovered with combinatorial synthesis. *Science* **1995**, *270*, 273–275.
- (29) Van Dover, R. B.; Schneemeyer, L. D.; Fleming, R. M. Discovery of a useful thin-film dielectric using a composition-spread approach. *Nature* **1998**, *392*, 162–164.
- (30) Senkan, S. M. High-throughput screening of solid-state catalyst libraries. *Nature* **1998**, *394*, 350–353.
- (31) Muster, T. H.; Trinchì, A.; Markley, T. A.; Lau, D.; Martin, P.; Bradbury, A.; Bendavid, A.; Dligatch, S. A review of high throughput and combinatorial electrochemistry. *Electrochim. Acta* **2011**, *56*, 9679–9699.
- (32) Sun, S.; Ding, J. J.; Bao, J.; Luo, Z. L.; Gao, C. Application of parallel synthesis and high throughput characterization in photocatalyst discovery. *Comb. Chem. High Throughput Screening* **2011**, *14*, 160–172.
- (33) Potyrailo, R. A.; Takeuchi, I. Role of high-throughput characterization tools in combinatorial materials science. *Meas. Sci. Technol.* **2005**, *16*, 1–4.
- (34) Takeuchi, I.; Lauterbach, J.; Fasolka, M. Combinatorial materials synthesis. *Mater. Today* **2005**, *8*, 18–26.
- (35) Jandeleit, B.; Schaefer, D. J.; Powers, T. S.; Turner, H. W.; Weinberg, W. H. Combinatorial materials science and catalysis. *Angew. Chem., Int. Ed.* **1999**, *38*, 2495–2532.
- (36) Woo, S. I.; Kim, K. W.; Cho, H. Y.; Oh, K. S.; Jeon, M. K.; Tarte, N. H.; Kim, T. S.; Mahmood, A. Current status of combinatorial and high-throughput methods for discovering new materials and catalysts. *QSAR Comb. Sci.* **2005**, *24*, 138–154.
- (37) Zhao, J. C. Combinatorial approaches as effective tools in the study of phase diagrams and composition-structure-property relationships. *Prog. Mater. Sci.* **2006**, *51*, 557–631.
- (38) Barber, Z. H.; Blamire, M. G. High throughput thin film materials science. *Mater. Sci. Technol.* **2008**, *24*, 757–770.
- (39) Takeuchi, I.; van Dover, R. B.; Koinuma, H. Combinatorial synthesis and evaluation of functional inorganic materials using thin-film techniques. *MRS Bull.* **2002**, *27*, 301–308.
- (40) Kafizas, A.; Parkin, I. P. Inorganic thin-film combinatorial studies for rapidly optimizing functional properties. *Chem. Soc. Rev.* **2012**, *41*, 738–81.
- (41) Fujishima, A.; Honda, K. Electrochemical photolysis of water at a semiconductor electrode. *Nature* **1972**, *238*, 37–38.
- (42) Teoh, W. Y.; Scott, J. A.; Amal, R. Progress in heterogeneous photocatalysis: From classical radical chemistry to engineering nanomaterials and solar reactors. *J. Phys. Chem. Lett.* **2012**, *3*, 629–639.
- (43) Pelizzetti, E. Convention on homogeneous and heterogeneous photocatalysis. *Chim. Ind. (Milan, Italy)* **1985**, *67*, 597–597.
- (44) Legrini, O.; Oliveros, E.; Braun, A. M. Photochemical processes for water-treatment. *Chem. Rev.* **1993**, *93*, 671–698.
- (45) Peyton Gary, R.; Glaze William, H. Mechanism of photolytic ozonation. In *Photochemistry of Environmental Aquatic Systems*; American Chemical Society: Washington, DC, 1987; Vol. 327, pp 76–88.
- (46) Tezcanli-Guyer, G.; Ince, N. H. Individual and combined effects of ultrasound, ozone and UV irradiation: A case study with textile dyes. *Ultrasonics* **2004**, *42*, 603–609.
- (47) Mills, A.; Le Hunte, S. An overview of semiconductor photocatalysis. *J. Photochem. Photobiol., A* **1997**, *108*, 1–35.
- (48) Choi, W. Y.; Termin, A.; Hoffmann, M. R. The role of metal-ion dopants in quantum-sized TiO₂: Correlation between photoreactivity and charge-carrier recombination dynamics. *J. Phys. Chem.* **1994**, *98*, 13669–13679.
- (49) Kamat, P. V. Photochemistry on nonreactive and reactive (semiconductor) surfaces. *Chem. Rev.* **1993**, *93*, 267–300.
- (50) Kamat, P. V. Manipulation of charge transfer across semiconductor interface. A criterion that cannot be ignored in photocatalyst design. *J. Phys. Chem. Lett.* **2012**, *3*, 663–672.
- (51) Kumar, S. G.; Devi, L. G. Review on modified TiO₂ photocatalysis under UV/visible light: Selected results and related mechanisms on interfacial charge carrier transfer dynamics. *J. Phys. Chem. A* **2011**, *115*, 13211–41.
- (52) Serpone, N.; Salinaro, A. Terminology, relative photonic efficiencies and quantum yields in heterogeneous photocatalysis. Part I: Suggested protocol (technical report). *Pure Appl. Chem.* **1999**, *71*, 303–320.
- (53) Gaya, U. I.; Abdullah, A. H. Heterogeneous photocatalytic degradation of organic contaminants over titanium dioxide: A review of fundamentals, progress and problems. *J. Photochem. Photobiol., C* **2008**, *9*, 1–12.
- (54) Glatzmaier, G. C.; Milne, T. A.; Tyner, C.; Sprung, J. Innovative solar technologies for treatment of concentrated organic wastes. *Sol. Energy Mater.* **1991**, *24*, 672–673.
- (55) Ollis, D. F.; Pelizzetti, E.; Serpone, N. Photocatalyzed destruction of water contaminants. *Environ. Sci. Technol.* **1991**, *25*, 1522–1529.
- (56) Yang, L. P.; Liu, Z. Y. Study on light intensity in the process of photocatalytic degradation of indoor gaseous formaldehyde for saving energy. *Energy Convers. Manage.* **2007**, *48*, 882–889.
- (57) Pareek, V.; Chong, S. H.; Tade, M.; Adesina, A. A. Light intensity distribution in heterogeneous photocatalytic reactors. *Asia-Pac. J. Chem. Eng.* **2008**, *3*, 171–201.
- (58) Curco, D.; Gimenez, J.; Addardak, A.; Cervera-March, S.; Eslugas, S. Effects of radiation absorption and catalyst concentration on the photocatalytic degradation of pollutants. *Catal. Today* **2002**, *76*, 177–188.
- (59) Wang, N.; Li, X. Y.; Wang, Y. X.; Quan, X.; Chen, G. H. Evaluation of bias potential enhanced photocatalytic degradation of 4-chlorophenol with TiO₂ nanotube fabricated by anodic oxidation method. *Chem. Eng. J.* **2009**, *146*, 30–35.
- (60) Quan, X.; Ruan, X. L.; Zhao, H. M.; Chen, S.; Zhao, Y. Z. Photoelectrocatalytic degradation of pentachlorophenol in aqueous solution using a TiO₂ nanotube film electrode. *Environ. Pollut.* **2007**, *147*, 409–414.
- (61) Malato, S.; Blanco, J.; Campos, A.; Caceres, J.; Guillard, C.; Herrmann, J. M.; Fernandez-Alba, A. R. Effect of operating parameters on the testing of new industrial titania catalysts at solar pilot plant scale. *Appl. Catal., B* **2003**, *42*, 349–357.
- (62) Fu, X. Z.; Clark, L. A.; Zeltner, W. A.; Anderson, M. A. Effects of reaction temperature and water vapor content on the heterogeneous photocatalytic oxidation of ethylene. *J. Photochem. Photobiol., A* **1996**, *97*, 181–186.
- (63) Wang, Y. B.; Hong, C. S. TiO₂-mediated photomineralization of 2-chlorobiphenyl: The role of O₂. *Water Res.* **2000**, *34*, 2791–2797.
- (64) Chong, M. N.; Jin, B.; Chow, C. W. K.; Saint, C. Recent developments in photocatalytic water treatment technology: A review. *Water Res.* **2010**, *44*, 2997–3027.
- (65) Dagher, R.; Drogué, P.; Robert, D. Photoelectrocatalytic technologies for environmental applications. *J. Photochem. Photobiol., A* **2012**, *238*, 41–52.
- (66) Bard, A. J. Photoelectrochemistry. *Science* **1980**, *207*, 139–144.
- (67) Sakai, T.; Kawai, T. Photosynthesis and photocatalysis with semiconductor powders. In *Energy Resources through Photochemistry and Catalysis*; Gratzel, M., Ed.; Academic Press, Inc.: New York, 1983; pp 332–358.
- (68) Gratzel, M. Photoelectrochemical cells. *Nature* **2001**, *414*, 338–344.

- (69) Nowotny, J.; Bak, T.; Nowotny, M. K.; Sheppard, L. R. Titanium dioxide for solar-hydrogen II. Defect chemistry. *Int. J. Hydrogen Energy* **2007**, *32*, 2630–2643.
- (70) Koelsch, M.; Cassaignon, S.; Minh, C. T. T.; Guillemoles, J. F.; Jolivet, J. P. Electrochemical comparative study of titania (anatase, brookite and rutile) nanoparticles synthesized in aqueous medium. *Thin Solid Films* **2004**, *451*, 86–92.
- (71) Asahi, R.; Taga, Y.; Mannstadt, W.; Freeman, A. J. Electronic and optical properties of anatase TiO₂. *Phys. Rev. B: Condens. Matter Mater. Phys.* **2000**, *61*, 7459–7465.
- (72) Stafford, U.; Gray, K. A.; Kamat, P. V.; Varma, A. An in situ diffuse reflectance FTIR investigation of photocatalytic degradation of 4-chlorophenol on a TiO₂ powder surface. *Chem. Phys. Lett.* **1993**, *205*, 55–61.
- (73) Jung, H. S.; Kim, H. Origin of low photocatalytic activity of rutile TiO₂. *Electron. Mater. Lett.* **2009**, *5*, 73–76.
- (74) Henglein, A. Photochemistry of colloidal cadmium-sulfide. 2. Effects of adsorbed methyl viologen and of colloidal platinum. *J. Phys. Chem.* **1982**, *86*, 2291–2293.
- (75) Reference Solar Spectral Irradiance: Air Mass 1.5. <http://rredc.nrel.gov/solar/spectra/am1.5/> (accessed on Sep 2012).
- (76) Wang, X. C.; Yu, J. C.; Ho, C. M.; Hou, Y. D.; Fu, X. Z. Photocatalytic activity of a hierarchically macro/mesoporous titania. *Langmuir* **2005**, *21*, 2552–2559.
- (77) Maira, A. J.; Yeung, K. L.; Lee, C. Y.; Yue, P. L.; Chan, C. K. Size effects in gas-phase photo-oxidation of trichloroethylene using nanometer-sized TiO₂ catalysts. *J. Catal.* **2000**, *192*, 185–196.
- (78) Antonietti, M.; Ozin, G. A. Promises and problems of mesoscale materials chemistry or why meso? *Chem. - Eur. J.* **2004**, *10*, 28–41.
- (79) Wang, D. H.; Ma, Z.; Dai, S.; Liu, J.; Nie, Z. M.; Engelhard, M. H.; Huo, Q. S.; Wang, C. M.; Kou, R. Low-temperature synthesis of tunable mesoporous crystalline transition metal oxides and applications as Au catalyst supports. *J. Phys. Chem. C* **2008**, *112*, 13499–13509.
- (80) Ryoo, R.; Joo, S. H.; Jun, S. Synthesis of highly ordered carbon molecular sieves via template-mediated structural transformation. *J. Phys. Chem. B* **1999**, *103*, 7743–7746.
- (81) Yu, J. G.; Su, Y. R.; Cheng, B. Template-free fabrication and enhanced photocatalytic activity of hierarchical macro-/mesoporous titania. *Adv. Funct. Mater.* **2007**, *17*, 1984–1990.
- (82) Chen, D. H.; Cao, L.; Huang, F. Z.; Imperia, P.; Cheng, Y. B.; Caruso, R. A. Synthesis of monodisperse mesoporous titania beads with controllable diameter, high surface areas, and variable pore diameters (14–23 nm). *J. Am. Chem. Soc.* **2010**, *132*, 4438–4444.
- (83) Li, H. X.; Bian, Z. F.; Zhu, J.; Zhang, D. Q.; Li, G. S.; Huo, Y. N.; Li, H.; Lu, Y. F. Mesoporous titania spheres with tunable chamber structure and enhanced photocatalytic activity. *J. Am. Chem. Soc.* **2007**, *129*, 8406–8407.
- (84) Mor, G. K.; Shankar, K.; Paulose, M.; Varghese, O. K.; Grimes, C. A. Use of highly-ordered TiO₂ nanotube arrays in dye-sensitized solar cells. *Nano Lett.* **2006**, *6*, 215–218.
- (85) Feng, X. J.; Shankar, K.; Varghese, O. K.; Paulose, M.; Latempa, T. J.; Grimes, C. A. Vertically aligned single crystal TiO₂ nanowire arrays grown directly on transparent conducting oxide coated glass: Synthesis details and applications. *Nano Lett.* **2008**, *8*, 3781–3786.
- (86) Miao, L.; Tanemura, S.; Toh, S.; Kaneko, K.; Tanemura, M. Fabrication, characterization and Raman study of anatase TiO₂ nanorods by a heating-sol-gel template process. *J. Cryst. Growth* **2004**, *264*, 246–252.
- (87) Rezaee, A.; Ghaneian, M. T.; Taghavinia, N.; Aminian, M. K.; Hashemian, S. J. TiO₂ nanofibre assisted photocatalytic degradation of Reactive Blue 19 dye from aqueous solution. *Environ. Technol.* **2009**, *30*, 233–239.
- (88) Fu, N.; Wu, Y. Q.; Jin, Z. L.; Lu, G. X. Structural-dependent photoactivities of TiO₂ nanoribbon for visible-light-induced H₂ evolution: The roles of nanocavities and alternate structures. *Langmuir* **2010**, *26*, 447–455.
- (89) Chen, X.; Mao, S. S. Titanium dioxide nanomaterials: Synthesis, properties, modifications, and applications. *Chem. Rev.* **2007**, *107*, 2891–2959.
- (90) Malato, S.; Fernandez-Ibanez, P.; Maldonado, M. I.; Blanco, J.; Gernjak, W. Decontamination and disinfection of water by solar photocatalysis: Recent overview and trends. *Catal. Today* **2009**, *147*, 1–59.
- (91) Litter, M. I. Heterogeneous photocatalysis: Transition metal ions in photocatalytic systems. *Appl. Catal., B* **1999**, *23*, 89–114.
- (92) Takeuchi, M.; Yamashita, H.; Matsuoka, M.; Anpo, M.; Hirao, T.; Itoh, N.; Iwamoto, N. Photocatalytic decomposition of NO under visible light irradiation on the Cr-ion-implanted TiO₂ thin film photocatalyst. *Catal. Lett.* **2000**, *67*, 135–137.
- (93) Kitano, M.; Matsuoka, M.; Ueshima, M.; Anpo, M. Recent developments in titanium oxide-based photocatalysts. *Appl. Catal., A* **2007**, *325*, 1–14.
- (94) Wang, X. D.; Waterhouse, G. I. N.; Mitchell, D. R. G.; Prince, K.; Caruso, R. A. Noble metal-modified porous titania networks and their application as photocatalysts. *ChemCatChem* **2011**, *3*, 1763–1771.
- (95) Pelaez, M.; Nolan, N. T.; Pillai, S. C.; Seery, M. K.; Falaras, P.; Kontos, A. G.; Dunlop, P. S. M.; Hamilton, J. W. J.; Byrne, J. A.; O'Shea, K.; Entezari, M. H.; Dionysiou, D. D. A review on the visible light active titanium dioxide photocatalysts for environmental applications. *Appl. Catal., B* **2012**, *125*, 331–349.
- (96) Irie, H.; Watanabe, Y.; Hashimoto, K. Carbon-doped anatase TiO₂ powders as a visible-light sensitive photocatalyst. *Chem. Lett.* **2003**, *32*, 772–773.
- (97) Morikawa, T.; Asahi, R.; Ohwaki, T.; Aoki, K.; Taga, Y. Band-gap narrowing of titanium dioxide by nitrogen doping. *Jpn. J. Appl. Phys. 2 Lett.* **2001**, *40*, L561–L563.
- (98) Han, C.; Pelaez, M.; Likodimos, V.; Kontos, A. G.; Falaras, P.; O'Shea, K.; Dionysiou, D. D. Innovative visible light-activated sulfur doped TiO₂ films for water treatment. *Appl. Catal., B* **2011**, *107*, 77–87.
- (99) Czoska, A. M.; Livraghi, S.; Chiesa, M.; Giamello, E.; Agnoli, S.; Granozzi, G.; Finazzi, E.; Di Valentin, C.; Pacchioni, G. The nature of defects in fluorine-doped TiO₂. *J. Phys. Chem. C* **2008**, *112*, 8951–8956.
- (100) Pelaez, M.; Falaras, P.; Likodimos, V.; Kontos, A. G.; de la Cruz, A. A.; O'Shea, K.; Dionysiou, D. D. Synthesis, structural characterization and evaluation of sol-gel-based NF-TiO₂ films with visible light-photoactivation for the removal of microcystin-LR. *Appl. Catal., B* **2010**, *99*, 378–387.
- (101) Etacheri, V.; Seery, M. K.; Hinder, S. J.; Pillai, S. C. Oxygen rich titania: A dopant free, high temperature stable, and visible-light active anatase photocatalyst. *Adv. Funct. Mater.* **2011**, *21*, 3744–3752.
- (102) Yu, Y.; Yu, J. C.; Yu, J. G.; Kwok, Y. C.; Che, Y. K.; Zhao, J. C.; Ding, L.; Ge, W. K.; Wong, P. K. Enhancement of photocatalytic activity of mesoporous TiO₂ by using carbon nanotubes. *Appl. Catal., A* **2005**, *289*, 186–196.
- (103) O'Regan, B.; Gratzel, M. A low-cost, high-efficiency solar-cell based on dye-sensitized colloidal TiO₂ films. *Nature* **1991**, *353*, 737–740.
- (104) Woodhouse, M.; Parkinson, B. A. Combinatorial approaches for the identification and optimization of oxide semiconductors for efficient solar photoelectrolysis. *Chem. Soc. Rev.* **2009**, *38*, 197–210.
- (105) Su, G. X.; Yan, B. Nano-combinatorial chemistry strategy for nanotechnology research. *J. Comb. Chem.* **2010**, *12*, 215–221.
- (106) Xiao, H. Y.; Dai, Q. X.; Li, W. S.; Au, C. T.; Zhou, X. P. Photodegradation catalyst screening by high throughput experiments. *J. Mol. Catal. A: Chem.* **2006**, *245*, 17–25.
- (107) Dai, Q.; Xiao, H.; Li, W.; Na, Y.; Zhou, X. Photodegradation catalyst screening by combinatorial methodology. *Appl. Catal., A* **2005**, *290*, 25–35.
- (108) Dai, Q. X.; Xiao, H. Y.; Li, W. S.; Na, Y. Q.; Zhou, X. P. Photodegradation catalyst discovery by high-throughput experiment. *J. Comb. Chem.* **2005**, *7*, 539–545.

- (109) Sohn, J. M.; Oh, K. S.; Woo, S. I. High-throughput screening of transition metal-doped TiO₂ in photodecomposition of phenol under visible light. *Korean J. Chem. Eng.* **2004**, *21*, 123–125.
- (110) Lettmann, C.; Hinrichs, H.; Maier, W. F. Combinatorial discovery of new photocatalysts for water purification with visible light. *Angew. Chem., Int. Ed.* **2001**, *40*, 3160–3164.
- (111) Seyler, M.; Stoewe, K.; Maier, W. F. New hydrogen-producing photocatalysts—A combinatorial search. *Appl. Catal., B* **2007**, *76*, 146–157.
- (112) Boldrin, P.; Hebb, A. K.; Chaudhry, A. A.; Otley, L.; Thiebaut, B.; Bishop, P.; Darr, J. A. Direct synthesis of nanosized NiCo₂O₄ spinel and related compounds via continuous hydrothermal synthesis methods. *Ind. Eng. Chem. Res.* **2007**, *46*, 4830–4838.
- (113) Adschiri, T.; Kanazawa, K.; Arai, K. Rapid and continuous hydrothermal crystallization of metal-oxide particles in supercritical water. *J. Am. Ceram. Soc.* **1992**, *75*, 1019–1022.
- (114) Chaudhry, A. A.; Haque, S.; Kellici, S.; Boldrin, P.; Rehman, I.; Fazal, A. K.; Darr, J. A. Instant nano-hydroxyapatite: A continuous and rapid hydrothermal synthesis. *Chem. Commun.* **2006**, 2286–2288.
- (115) Thompson, K.; Goodall, J.; Kellici, S.; Mattinson, J. A.; Egerton, T. A.; Rehman, I.; Darr, J. A. Screening tests for the evaluation of nanoparticle titania photocatalysts. *J. Chem. Technol. Biotechnol.* **2009**, *84*, 1717–1725.
- (116) Nagaveni, K.; Hegde, M. S.; Madras, G. Structure and photocatalytic activity of Ti_{1-x}M_xO_{2±δ} (M = W, V, Ce, Zr, Fe, and Cu) synthesized by solution combustion method. *J. Phys. Chem. B* **2004**, *108*, 20204–20212.
- (117) Nagaveni, K.; Hegde, M. S.; Ravishankar, N.; Subbanna, G. N.; Madras, G. Synthesis and structure of nanocrystalline TiO₂ with lower band gap showing high photocatalytic activity. *Langmuir* **2004**, *20*, 2900–2907.
- (118) Nagaveni, K.; Sivalingam, G.; Hegde, M. S.; Madras, G. Photocatalytic degradation of organic compounds over combustion-synthesized nano-TiO₂. *Environ. Sci. Technol.* **2004**, *38*, 1600–1604.
- (119) Luo, Z. L.; Geng, B.; Bao, J.; Gao, C. Parallel solution combustion synthesis for combinatorial materials studies. *J. Comb. Chem.* **2005**, *7*, 942–946.
- (120) Ding, J. J.; Bao, J.; Sun, S. N.; Luo, Z. L.; Gao, C. Combinatorial discovery of visible-light driven photocatalysts based on the ABO₃-type (A = Y, La, Nd, Sm, Eu, Gd, Dy, Yb, B = Al and In) binary oxides. *J. Comb. Chem.* **2009**, *11*, 523–526.
- (121) Dhumal, S. Y.; Daulton, T. L.; Jiang, J.; Khomami, B.; Biswas, P. Synthesis of visible light-active nanostructured TiO_x (x < 2) photocatalysts in a flame aerosol reactor. *Appl. Catal., B* **2009**, *86*, 145–151.
- (122) Chen, L.; Bao, J.; Gao, C.; et al. Combinatorial synthesis of insoluble oxide library from ultrafine/nano particle suspension using a drop-on-demand inkjet delivery system. *J. Comb. Chem.* **2004**, *6*, 699–702.
- (123) Nakayama, A.; Suzuki, E.; Ohmori, T. Development of high throughput evaluation for photocatalyst thin-film. *Appl. Surf. Sci.* **2002**, *189*, 260–264.
- (124) Kafizas, A.; Parkin, I. P. The combinatorial atmospheric pressure chemical vapour deposition (cAPCVD) of a grading N-doped mixed phase titania thin film. *J. Mater. Chem.* **2010**, *20*, 2157–2169.
- (125) Guerin, S.; Hayden, B. E. Physical vapor deposition method for the high-throughput synthesis of solid-state material libraries. *J. Comb. Chem.* **2006**, *8*, 66–73.
- (126) Arai, T.; Konishi, Y.; Iwasaki, Y.; Sugihara, H.; Sayama, K. High-throughput screening using porous photoelectrode for the development of visible-light-responsive semiconductors. *J. Comb. Chem.* **2007**, *9*, 574–581.
- (127) Woodhouse, M.; Herman, G. S.; Parkinson, B. A. Combinatorial approach to identification of catalysts for the photoelectrolysis of water. *Chem. Mater.* **2005**, *17*, 4318–4324.
- (128) Okimura, K.; Maeda, N.; Shibata, A. Characteristics of rutile TiO₂ films prepared by rf magnetron sputtering at a low temperature. *Thin Solid Films* **1996**, *282*, 427–430.
- (129) Rodriguez, J.; Gomez, M.; Ederth, J.; Niklasson, G. A.; Granqvist, C. G. Thickness dependence of the optical properties of sputter deposited Ti oxide films. *Thin Solid Films* **2000**, *365*, 119–125.
- (130) Rodriguez, J.; Gomez, M.; Lindquist, S. E.; Granqvist, C. G. Photo-electrocatalytic degradation of 4-chlorophenol over sputter deposited Ti oxide films. *Thin Solid Films* **2000**, *360*, 250–255.
- (131) Matsumoto, Y.; Murakami, M.; Jin, Z. W.; Ohtomo, A.; Lippmaa, M.; Kawasaki, M.; Koinuma, H. Combinatorial laser molecular beam epitaxy (MBE) growth of Mg-Zn-O alloy for band gap engineering. *Jpn. J. Appl. Phys. 2 Lett.* **1999**, *38*, L603–L605.
- (132) Koinuma, H.; Koida, T.; Ohnishi, T.; Komiyama, D.; Lippmaa, M.; Kawasaki, M. Parallel fabrication of artificially designed superlattices by combinatorial laser MBE. *Appl. Phys. A: Mater. Sci. Process.* **1999**, *69*, S29–S31.
- (133) Koinuma, H.; Takeuchi, I. Combinatorial solid-state chemistry of inorganic materials. *Nat. Mater.* **2004**, *3*, 429–438.
- (134) Koinuma, H. Quantum functional oxides and combinatorial chemistry. *Solid State Ionics* **1998**, *108*, 1–7.
- (135) Matsumoto, Y.; Murakami, M.; Jin, Z. W.; Nakayama, A.; Yamaguchi, T.; Ohmori, T.; Suzuki, E.; Nomura, S.; Kawasaki, M.; Koinuma, H. Combinatorial synthesis and high throughput evaluation of doped TiO₂ thin films for the development of photocatalysts. In *Combinatorial and Composition Spread Techniques in Materials and Device Development*; Jabbar, G. E., Ed.; SPIE: San Jose, CA, 2000; Vol. 3941, pp 19–27.
- (136) Koinuma, H.; Itaka, K.; Matsumoto, Y.; Yoshida, Y.; Aikawa, S.; Takeuchi, K. Vacuum and pressured combinatorial processings for exploration of environmental catalysts. *Top. Catal.* **2010**, *53*, 35–39.
- (137) Hyett, G.; Green, M.; Parkin, I. P. X-ray diffraction area mapping of preferred orientation and phase change in TiO₂ thin films deposited by chemical vapor deposition. *J. Am. Chem. Soc.* **2006**, *128*, 12147–12155.
- (138) Kafizas, A.; Adriaens, D.; Mills, A.; Parkin, I. P. Simple method for the rapid simultaneous screening of photocatalytic activity over multiple positions of self-cleaning films. *Phys. Chem. Chem. Phys.* **2009**, *11*, 8367–8375.
- (139) Kafizas, A.; Parkin, I. P. Combinatorial atmospheric pressure chemical vapor deposition (cAPCVD): A route to functional property optimization. *J. Am. Chem. Soc.* **2011**, *133*, 20458–20467.
- (140) Chadwick, N.; Sathasivam, S.; Kafizas, A.; Bawaked, S. M.; Obaid, A. Y.; Al-Thabaiti, S.; Basahel, S. N.; Parkin, I. P.; Carmalt, C. J. Combinatorial aerosol assisted chemical vapour deposition of a photocatalytic mixed SnO₂/TiO₂ thin film. *J. Mater. Chem. A* **2014**, *2*, 5108–5116.
- (141) Baeck, S.-H.; Jaramillo, T. F.; Kleiman-Shwarsstein, A.; McFarland, E. W. Automated electrochemical synthesis and characterization of TiO₂ supported Au nanoparticle electrocatalysts. *Meas. Sci. Technol.* **2005**, *16*, 54–59.
- (142) Brandli, C.; Jaramillo, T. F.; Ivanovskaya, A.; McFarland, E. W. Automated synthesis and characterization of diverse libraries of macroporous alumina. *Electrochim. Acta* **2001**, *47*, 553–557.
- (143) Jaramillo, T. F.; Ivanovskaya, A.; McFarland, E. W. High-throughput screening system for catalytic hydrogen-producing materials. *J. Comb. Chem.* **2002**, *4*, 17–22.
- (144) Baeck, S. H.; Jaramillo, T. F.; Brandli, C.; McFarland, E. W. Combinatorial electrochemical synthesis and characterization of tungsten-based mixed-metal oxides. *J. Comb. Chem.* **2002**, *4*, 563–568.
- (145) Jaramillo, T. F.; Baeck, S. H.; Kleiman-Shwarsstein, A.; McFarland, E. W. Combinatorial electrochemical synthesis and screening of mesoporous ZnO for photocatalysis. *Macromol. Rapid Commun.* **2004**, *25*, 297–301.
- (146) Liu, X.; Shen, Y.; Yang, R.; Zou, S.; Ji, X.; Shi, L.; Zhang, Y.; Liu, D.; Xiao, L.; Zheng, X.; Li, S.; Fan, J.; Stucky, G. D. Inkjet printing assisted synthesis of multicomponent mesoporous metal oxides for ultrafast catalyst exploration. *Nano Lett.* **2012**, *12*, 5733–5739.
- (147) Du, P.; Buenolopez, A.; Verbaas, M.; Almeida, A.; Makkee, M.; Mouljijn, J.; Mul, G. The effect of surface OH-population on the photocatalytic activity of rare earth-doped P25-TiO₂ in methylene blue degradation. *J. Catal.* **2008**, *260*, 75–80.

- (148) Ritter, A.; Reifler, F. A.; Saini, S. Quick screening method for the photocatalytic activity of nanoparticles and powdery materials. *Appl. Catal., A* **2009**, *352*, 271–276.
- (149) Zou, Z. J.; Liu, Y.; Li, H. Y.; Liao, Y. C.; Xie, C. S. Synthesis of TiO₂/WO₃/MnO₂ composites and high-throughput screening for their photoelectrical properties. *J. Comb. Chem.* **2010**, *12*, 363–369.
- (150) Schmidt, H.; Akarsu, M.; Muller, T. S.; Moh, K.; Schafer, G.; Strauss, D. J.; Naumann, M. The formation of gradients in wet deposited coatings with photocatalytically active nanoparticles. *Res. Chem. Intermed.* **2005**, *31*, 535–553.
- (151) Ohtani, B. Photocatalysis A to Z—What we know and what we do not know in a scientific sense. *J. Photochem. Photobiol., C* **2010**, *11*, 157–178.
- (152) O'Rourke, C.; Mills, A. Adsorption and photocatalytic bleaching of acid orange 7 on P25 titania. *J. Photochem. Photobiol., A* **2010**, *216*, 261–267.
- (153) Yan, X. L.; Ohno, T.; Nishijima, K.; Abe, R.; Ohtani, B. Is methylene blue an appropriate substrate for a photocatalytic activity test? A study with visible-light responsive titania. *Chem. Phys. Lett.* **2006**, *429*, 606–610.
- (154) Mills, A.; Hill, C.; Robertson, P. K. J. Overview of the current ISO tests for photocatalytic materials. *J. Photochem. Photobiol., A* **2012**, *237*, 7–23.
- (155) Ritter, A.; Reifler, F. A.; Michel, E. Quick screening method for the photocatalytic activity of textile fibers and fabrics. *Text. Res. J.* **2010**, *80*, 604–610.
- (156) Potyrailo, R. A.; Pickett, J. E. High-throughput multilevel performance screening of advanced materials. *Angew. Chem., Int. Ed.* **2002**, *41*, 4230–4233.
- (157) Morris, N. D.; Mallouk, T. E. A high-throughput optical screening method for the optimization of colloidal water oxidation catalysts. *J. Am. Chem. Soc.* **2002**, *124*, 11114–11121.
- (158) Mills, A.; McGrady, M.; Wang, J.; Hepburn, J. A rapid method of assessing the photocatalytic activity of thin TiO₂ films using an ink based on the redox dye 2,6-dichloroindophenol. *Int. J. Photoenergy* **2008**, *2008*, 1.
- (159) Liao, Y. C.; Li, H. Y.; Liu, Y. A.; Zou, Z. J.; Zeng, D. W.; Xie, C. S. Characterization of photoelectric properties and composition effect of TiO₂/ZnO/Fe₂O₃ composite by combinatorial methodology. *J. Comb. Chem.* **2010**, *12*, 883–889.
- (160) Luo, Z. L.; Geng, B.; Bao, J.; Liu, C. H.; Liu, W. H.; Gao, C.; Liu, Z. G.; Ding, X. L. High-throughput x-ray characterization system for combinatorial materials studies. *Rev. Sci. Instrum.* **2005**, *76*, 095105.
- (161) Isaacs, E. D.; Marcus, M.; Aeppli, G.; Xiang, X. D.; Sun, X. D.; Schultz, P.; Kao, H. K.; Cargill, G. S.; Haushalter, R. Synchrotron x-ray microbeam diagnostics of combinatorial synthesis. *Appl. Phys. Lett.* **1998**, *73*, 1820–1822.
- (162) Ohtani, M.; Fukumura, T.; Kawasaki, M.; Omote, K.; Kikuchi, T.; Harada, J.; Ohtomo, A.; Lippmaa, M.; Ohnishi, T.; Komiyama, D.; Takahashi, R.; Matsumoto, Y.; Koinuma, H. Concurrent x-ray diffractometer for high throughput structural diagnosis of epitaxial thin films. *Appl. Phys. Lett.* **2001**, *79*, 3594–3596.
- (163) Barr, G.; Dong, W.; Gilmore, C. J. High-throughput powder diffraction. II. Applications of clustering methods and multivariate data analysis. *J. Appl. Crystallogr.* **2004**, *37*, 243–252.
- (164) Gregoire, J. M.; Dale, D.; Kazimirov, A.; DiSalvo, F. J.; van Dover, R. B. High energy X-ray diffraction/X-ray fluorescence spectroscopy for high-throughput analysis of composition spread thin films. *Rev. Sci. Instrum.* **2009**, *80*, 123905.
- (165) Kukuruznyak, D. A.; Reichert, H.; Okasinski, J.; Dosch, H.; Chikyow, T.; Daniels, J.; Honkimaki, V. High-throughput screening of combinatorial materials libraries by high-energy x-ray diffraction. *Appl. Phys. Lett.* **2007**, *91*, 071916.
- (166) Moates, F. C.; Somani, M.; Annamalai, J.; Richardson, J. T.; Luss, D.; Willson, R. C. Infrared thermographic screening of combinatorial libraries of heterogeneous catalysts. *Ind. Eng. Chem. Res.* **1996**, *35*, 4801–4803.
- (167) Holzwarth, A.; Schmidt, P. W.; Maier, W. E. Detection of catalytic activity in combinatorial libraries of heterogeneous catalysts by IR thermography. *Angew. Chem., Int. Ed.* **1998**, *37*, 2644–2647.
- (168) Scheidtmann, J.; Weiss, P. A.; Maier, W. F. Hunting for better catalysts and materials-combinatorial chemistry and high throughput technology. *Appl. Catal., A* **2001**, *222*, 79–89.
- (169) Loskyll, J.; Stoewe, K.; Maier, W. F. Infrared thermography as a high-throughput tool in catalysis research. *ACS Comb. Sci.* **2012**, *14*, 295–303.
- (170) Snively, C. M.; Oskarsdottir, G.; Lauterbach, J. Chemically sensitive high throughput parallel analysis of solid phase supported library members. *J. Comb. Chem.* **2000**, *2*, 243–245.
- (171) Snively, C. M.; Oskarsdottir, G.; Lauterbach, J. Chemically sensitive parallel analysis of combinatorial catalyst libraries. *Catal. Today* **2001**, *67*, 357–368.
- (172) Kassem, M.; Senkan, S. M. Chemical-structure of fuel-rich 1,2-C₂H₄Cl₂/CH₄/O₂/Ar flames: Effects of micro-probe cooling on the sampling of flames of chlorinated hydrocarbons. *Combust. Sci. Technol.* **1986**, *67*, 147–157.
- (173) Wang, H.; Liu, Z. M.; Shen, J. H. Quantified MS analysis applied to combinatorial heterogeneous catalyst libraries. *J. Comb. Chem.* **2003**, *5*, 802–808.
- (174) Hahndorf, I.; Buyevskaya, O.; Langpape, M.; Grubert, G.; Kolf, S.; Guillon, E.; Baerns, M. Experimental equipment for high-throughput synthesis and testing of catalytic materials. *Chem. Eng. J.* **2002**, *89*, 119–125.
- (175) Shapiro, M. J.; Gounarides, J. S. NMR methods utilized in combinatorial chemistry research. *Prog. Nucl. Magn. Reson. Spectrosc.* **1999**, *35*, 153–200.